

Molina, Renato; Villaseñor-Derbez, Juan Carlos; McDonald, Gavin; McDermott, Grant

Working Paper

Dangerous Waters: The Economic Toll of Piracy on Maritime Shipping

CESifo Working Paper, No. 11077

Provided in Cooperation with:

Ifo Institute – Leibniz Institute for Economic Research at the University of Munich

Suggested Citation: Molina, Renato; Villaseñor-Derbez, Juan Carlos; McDonald, Gavin; McDermott, Grant (2024) : Dangerous Waters: The Economic Toll of Piracy on Maritime Shipping, CESifo Working Paper, No. 11077, Center for Economic Studies and ifo Institute (CESifo), Munich

This Version is available at:

<https://hdl.handle.net/10419/296166>

Standard-Nutzungsbedingungen:

Die Dokumente auf EconStor dürfen zu eigenen wissenschaftlichen Zwecken und zum Privatgebrauch gespeichert und kopiert werden.

Sie dürfen die Dokumente nicht für öffentliche oder kommerzielle Zwecke vervielfältigen, öffentlich ausstellen, öffentlich zugänglich machen, vertreiben oder anderweitig nutzen.

Sofern die Verfasser die Dokumente unter Open-Content-Lizenzen (insbesondere CC-Lizenzen) zur Verfügung gestellt haben sollten, gelten abweichend von diesen Nutzungsbedingungen die in der dort genannten Lizenz gewährten Nutzungsrechte.

Terms of use:

Documents in EconStor may be saved and copied for your personal and scholarly purposes.

You are not to copy documents for public or commercial purposes, to exhibit the documents publicly, to make them publicly available on the internet, or to distribute or otherwise use the documents in public.

If the documents have been made available under an Open Content Licence (especially Creative Commons Licences), you may exercise further usage rights as specified in the indicated licence.

Dangerous Waters: The Economic Toll of Piracy on Maritime Shipping

*Renato Molina, Juan Carlos Villaseñor-Derbez, Gavin McDonald,
Grant McDermott*

Impressum:

CESifo Working Papers

ISSN 2364-1428 (electronic version)

Publisher and distributor: Munich Society for the Promotion of Economic Research - CESifo GmbH

The international platform of Ludwigs-Maximilians University's Center for Economic Studies and the ifo Institute

Poschingerstr. 5, 81679 Munich, Germany

Telephone +49 (0)89 2180-2740, Telefax +49 (0)89 2180-17845, email office@cesifo.de

Editor: Clemens Fuest

<https://www.cesifo.org/en/wp>

An electronic version of the paper may be downloaded

- from the SSRN website: www.SSRN.com
- from the RePEc website: www.RePEc.org
- from the CESifo website: <https://www.cesifo.org/en/wp>

Dangerous Waters: The Economic Toll of Piracy on Maritime Shipping

Abstract

Maritime transport has been historically susceptible to piracy. While broad assessments suggest the impact of modern piracy causes large economic losses, the literature lacks quantification of the magnitude of the costs and the behavioral responses that underpin them. Here, we combine theory and a unique geospatial dataset combining more than 25 million shipping voyages and thousands of pirate encounters across the globe to find that pirate encounters lead to significant and costly avoidance measures. Shippers modify their path along a route to avoid locations with known pirate encounters. This increases voyage distance and duration, which lead to significant increases in fuel and labor costs estimated to be over US\$1.5 billion/year. Additionally, emission of CO₂, NO_x, and SO_x due to increased fuel consumption results in environmental damages valued at US\$5.1 billion per year. Together, our results provide the first global estimates linking the presence of pirates to individual behaviour and aggregate transportation cost, as well as its environmental impact, with major implications for the shipping industry and maritime security at a global scale.

JEL-Codes: Q500, F500, R400.

Keywords: piracy, shipping, avoidance.

*Renato Molina**

*Department of Environmental Science and
Policy & Department of Economics
University of Miami / FL / USA
renato.molina@miami.edu*

Juan Carlos Villaseñor-Derbez

*Oceans Department, Doerr School of
Sustainability, Stanford University
Stanford / CA / USA
juancvd@stanford.edu*

Gavin McDonald

*Marine Science Institute, Bren School of
Environmental Science & Management,
Environmental Markets Lab, University of
California, Santa Barbara / USA
gmcdonald@bren.ucsb.edu*

Grant McDermott

*Department of Economics
University of Oregon
Eugene / OR / USA
gmcd@amazon.com*

*corresponding author

Preliminary work. All errors are our own.

“As by means of water-carriage, a more extensive market is opened to every sort of industry than what land-carriage alone can afford it”

–Adam Smith, *the Wealth of Nations*

20 **Introduction**

21 As it has done for centuries, maritime transport provides the main conduit for the world’s trading
22 activities. The oceans today carry more than 70% of globally traded goods by value and more
23 than 80% by volume (1). However, the industry remains susceptible to the threat of piracy.
24 Piracy grabbed worldwide headlines during the late 2000s, after a sharp increase in violent
25 encounters off the coast of Somalia. A recurring spate of attacks since then have disrupted
26 key shipping routes worldwide, most recently the Gulf of Aden. Despite these ongoing and
27 growing concerns, only limited efforts have been devoted to assess the behavioral underpinnings
28 of modern-day piracy and its underlying mechanisms, and ultimately its economic costs and
29 environmental impacts.

30 Historically coinciding with the earliest records of trade, the transportation of goods and the
31 difficulty of enforcement has always offered an opportunity for pirates to predate on commerce
32 routes (2). Maritime routes are particularly susceptible because they offer unique opportunities

33 for ambush and escape. In addition, they often lack clear jurisdictions, which complicates
34 capture and prosecution.¹ Beyond folklore and their occasionally romanticized origins, pirates
35 remain a relevant problem today. Official global records point to more than 2,200 pirate attacks
36 between 2013 and 2021, with 232 taking place in 2021 alone. Previous efforts to quantify the
37 cost of this problem suggest annual losses in excess of US\$20 billion/year (6, 7), although the
38 mechanics behind these costs are not always clearly specified (see Supplementary Text S2.1
39 for additional background on global piracy and an associated literature review). Something
40 that is clear, however, is that most encounters concentrate in busy trade channels, where pirates
41 target high-value vessels for robbery or capture-to-ransom (8). In this paper, we focus on three
42 “hotspots”—the Gulf of Aden, the Gulf of Guinea, and the Malacca Strait in Southeast Asia—
43 where piracy attacks have been particularly acute (Figure 1).

44 When deterrence or other enforcement options are too costly, then adaptation remains the
45 best course of action for individual vessels facing a piracy threat. How might shippers respond
46 to information of pirate presence along their route? Consider an example of change in shipping
47 behavior following news of a pirate encounter in the Makassar Strait, Indonesia. On June 19,
48 2013 a Hong Kong-flagged bulk carrier was boarded by three to five robbers. Information on
49 the attack was broadcast to other vessels in the region via the Anti-shipping Activity Messages
50 (ASAM) communication network, allowing them to modify their routes.² Per Figure 2, there

¹Historians point out that piracy often follows a well defined cycle involving a group of individuals from impoverished coastal areas that would band to predate on small-scale, poorly enforced shipments. These groups would then transition to a state of adjustment, for which “competition” dictates profitability and thereby their longevity in the piracy business (2, 3). Most of these observations are based on pirates from previous centuries, but the resemblance with modern pirates is evident. See Bahadur (4) and Bueger (5) for a detailed account of the cycle and organizational mechanisms in the case of the pirates of Somalia, which resembles very closely the documented paths for earlier pirates.

²The Worldwide Threat to Shipping Report reads: *On 19 June, the anchored Hong Kong-flagged bulk carrier OCEAN GARNET was boarded at 01-11S 117-12E, at the Muara Jawa Anchorage, Samarinda. Deck watch keepers onboard the anchored bulk carrier noticed three to five robbers with long knives near the forecandle store. They raised the alarm and retreated into the accommodation. On hearing the alarm, the robbers escaped in their waiting boat. Upon investigation, it was discovered that ship’s stores had been stolen. Port control was informed.* The entry is available at <https://t.ly/bsNk7> [Last visited on 04/12/24]

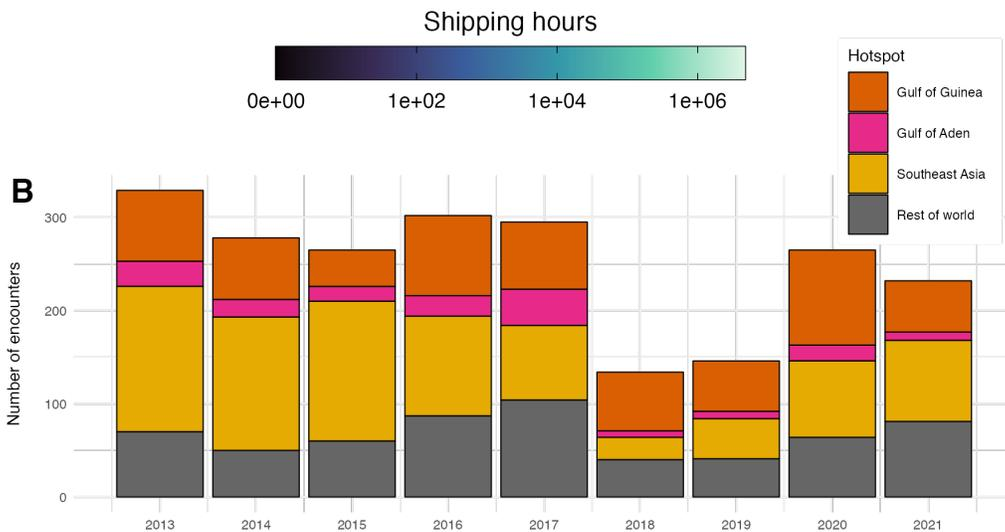
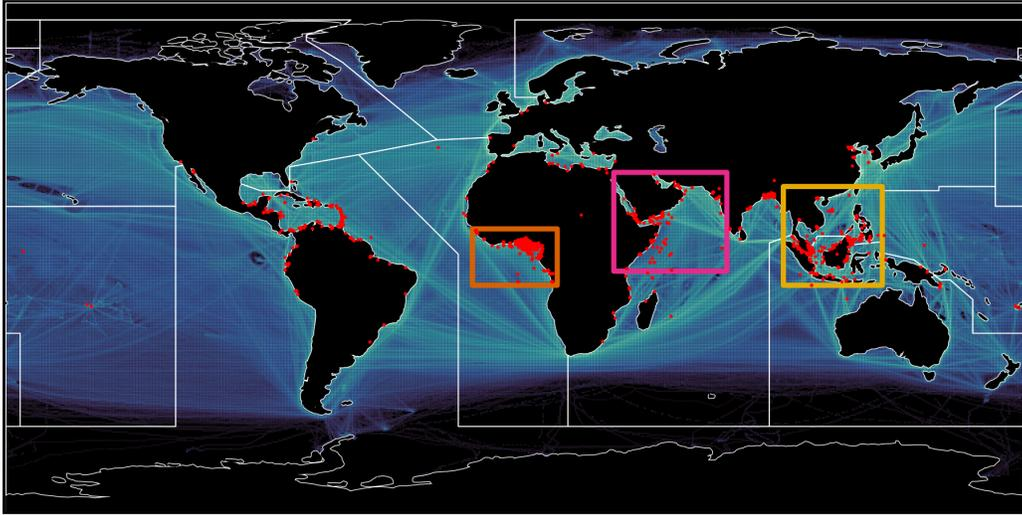
A

Fig 1: A global view of modern-day maritime transport and piracy. Panel A shows the spatial overlap of shipping activity and anti-shiping encounters from 2013 to 2021. Note that data are \log_{10} -transformed for visualization purposes and represented using a $0.5^\circ \times 0.5^\circ$ grid in geographic coordinates, with the fill color of each pixel represents the total shipping transit time from 2013-2021 (hr). Pirate encounters are shown as red points. The colored overlay bounding rectangles correspond to the three main piracy hotspots, namely: 1) Gulf of Guinea, 2) Gulf of Aden, and 3) Southeast Asia. The bounding boxes are defined by an empirical density-based clustering approach (see Materials and Methods). Outlines of the major Anti-shiping Activity Messages (ASAM) regions are shown as white lines. Panel B shows a number of pirate encounters across hotspots and the rest of the world from 2013 to 2021.

51 is a near-total avoidance of the attack area following the ASAM broadcast; the previous cluster
 52 of shipping activity near the Muara Jawa Anchorage all but disappeared and was replaced by a
 53 new one further South (Panel A). The number of voyages in the affected area also dropped from
 54 an average of 48 per day to just 3 per day (Panel B).

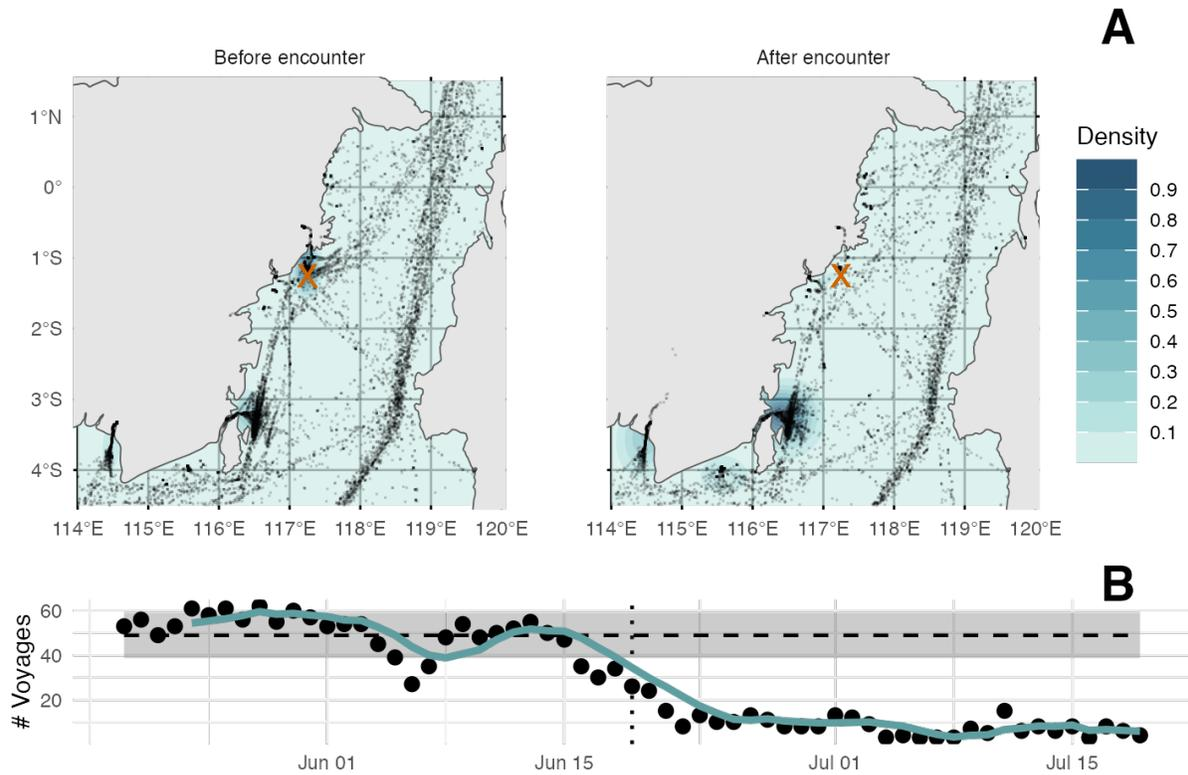


Fig 2: **Example of change in shipping vessel transit following an encounter with pirates on June 19, 2013 off the coast of Indonesia.** Panel A shows maps of the Muara Jawa Anchorage before (left) and after (right) the encounter. “X” marks the spot of the encounter. Points show all vessel positions recorded one week before or after the attack, and background colors show a 2-dimensional kernel estimate of vessel density. Panel B shows a time series of daily number of voyages crossing the affected grid cell (at 117E, 1.5S, indicated with an orange “X” in A). Each point shows the total daily number of voyages, and the blue line shows the mean number in a 5-day rolling window. The horizontal dashed line and shaded area show the baseline number of daily voyages (mean \pm standard-deviation) before the attack.

55 The contributions of this paper are threefold. First, we develop a formal theoretical model
 56 that explains the optimal avoidance behaviour of individual vessels following incidents like the

57 2013 Makassar Strait attack. Second, we test our model predictions on a rich dataset that com-
58 bines detailed voyage information with piracy events. Third, we determine the aggregate costs
59 that can be attributed to recent pirate attacks and the knock-on effects on vessel behavior and
60 global shipping. We achieve these goals by merging theoretical insights with data on shipping
61 voyages and pirate encounters to credibly assess the causal effect of piracy on the shipping in-
62 dustry. We formalize the decision-making process of sea captains based on warning reports, and
63 compile a unique geospatial dataset to test those insights. The dataset includes high resolution
64 spatio-temporal information on pirate encounters from the US National Geospatial Intelligence
65 Agency ASAM database,³ as well as individual vessel tracks of all known cargo, tanker, and
66 refrigerated vessels that use Automatic Identification System (AIS) due to (9). Our empirical
67 results show that a pirate encounter along a shipping route causes vessels to extend their trips
68 by an average of 28 (± 45) kilometers in the subsequent months, as they engage in avoidance
69 behavior. When aggregated at the industry level, and taking into account prevailing fuel and
70 labour costs, these adjustments suggest additional transportation costs of US\$1.7 billion as of
71 2021. Moreover, we estimate that surplus emission of air pollutants (CO_2 , NO_x , and SO_x) due to
72 increased fuel usage results in an additional cost of US\$5.1 billion in environmental damages.
73 These estimates highlight a previously undocumented loss in terms of operational cost, but also
74 in terms of global fuel consumption and the associated added emissions of both greenhouse
75 gasses and local pollutants.

³Information reported as The Worldwide Threats to Shipping Report by Office of Naval Intelligence. Recent reports are available at [Last checked 04/12/24]

76 **Results**

77 **A model of pirates and shippers**

78 To guide our empirical analysis, we propose a theoretical framework that characterizes rational
79 avoidance behavior under the threat of piracy. The model details, derivations and proofs are pro-
80 vided in Supplementary Text S2.2. Summarizing, the model yields three high-level and testable
81 predictions. First, shippers will never ignore the threat of piracy. Second, they will avoid pi-
82 rates following an assessment of the relative costs of partial and total avoidance, which in turn is
83 based on their potential shipping route(s) and their beliefs about the pirates' capabilities. Third,
84 shippers will incorporate past pirate encounters to inform their avoidance decisions.

85 With these testable predictions in hand, and to avoid ambiguity, it will prove helpful to
86 define precisely several terms that we use in our empirical analysis. A *route* is a port-to-port
87 combination, a *voyage* is a trip made along a route, and a *path* is the sequence of coordinates
88 chosen by the vessel to travel a route.

89 **Empirical evidence of behavioral adjustments by shippers**

90 Our theory model predicts vessel captains will adjust their paths along a route if they receive
91 new information about the risk of a piracy attack. Just as we saw in Figure 2, this implies that
92 a piracy-afflicted region will receive fewer transits, in expectation, after an attack. We evaluate
93 this prediction empirically by testing for systematic changes in daily transit activity within
94 all $0.5^\circ \times 0.5^\circ$ grid cells that experienced reported pirate activity between 2013 and 2021 (see
95 Supplementary Text S2.4 for detailed summary statistics). The results are displayed in Table 1.
96 Summarizing, we find that an additional pirate encounter within the preceding 90 days generally
97 leads to a significant reduction in vessel activity within the affected grid cell. This finding
98 holds across a variety of transit measures across all three of our designated hotspot regions. For
99 example, a piracy event in the Gulf of Aden correlates to 26.5 fewer kilometers traveled through

100 each grid cell within the region during the subsequent three months, as well as 0.7 fewer hours of
101 travel time, and approximately 0.6 fewer voyages and vessels passing through. The equivalent
102 impacts are less pronounced in magnitude for the Gulf of Guinea and southeast Asia. However,
103 the negative coefficients remain statistically significant for these other hotspots too. The picture
104 is murkier when zooming up to the global level and possibly reflects a reallocation (spillover)
105 effect between regions and routes for which it is difficult to control. Regardless, and while we
106 do not observe statistically significant coefficients for the global sample, these results are robust
107 to a variety of specification and data checks (see Supplementary Text S2.7.1).

108 Moving beyond grid-level impacts, how do these adjustments manifest at the level of in-
109 dividual voyages? Bearing in mind the empirical challenges described in Supplementary Text
110 S2.3, we test for changes in core voyage characteristics in Table 2. Summarizing, we observe
111 that a piracy encounter along a vessel's likely voyage path leads to longer average travel dis-
112 tances and prolonged travel times (summary statistics are available in the Supplementary Text
113 S2.4). The global estimate suggests that an additional pirate encounter within the preceding
114 three months translates to respective increases of 27.83 km in distance and 2.25 hrs in travel
115 time along a given route. We find consistent results when restricting the sample to voyages that
116 traverse hotspots, although the effect is much more pronounced for voyages passing through
117 the Gulf of Aden (210.9 km and 10.44 hr, respectively). Supplementary Text S2.6 includes an
118 auxiliary analysis using instrumental variables that corroborates the results presented here.

119 In contrast to the economically meaningful impacts on travel distance and time, the effect
120 on speed is minimal. We interpret these results as an indication that adjustments to speed
121 are a less cost-effective avoidance measure, or technically infeasible due to engine and vessel
122 limitations. This behavior is consistent with optimal avoidance since the cost of each additional
123 unit of distance traveled grows linearly, while the cost per each additional unit of cruising speed
124 grows exponentially (*10*). These results are robust to specification, subsampling, and data

Table 1: Effect of Piracy on Grid-level Ship Transit.

	Global	G. of Aden	G. of Guinea	S.E. Asia
<i>Panel (A): Total Distance (km)</i>				
Encounters (3 mo)	-4.90 (11.53)	-26.50* (13.78)	-4.58*** (1.32)	-3.69 (21.18)
Observations	1,939,330	305,691	440,458	489,763
<i>Panel (B): Occupancy (hr)</i>				
Encounters (3 mo)	8.42 (6.73)	-0.70 (1.20)	-0.26 (0.62)	15.97 (9.89)
Observations	1,939,330	305,691	440,458	489,763
<i>Panel (C): Voyages (#)</i>				
Encounters (3 mo)	0.32 (0.44)	-0.67** (0.34)	-0.11*** (0.04)	0.79 (0.68)
Observations	1,939,330	305,691	440,458	489,763
<i>Panel (D): Vessels (#)</i>				
Encounters (3 mo)	0.35 (0.45)	-0.65* (0.34)	-0.10*** (0.04)	0.83 (0.69)
Observations	1,939,330	305,691	440,458	489,763

* $p < 0.1$, ** $p < 0.05$, *** $p < 0.01$ The unit of observation is a grid cell ($N = 590$ unique cells). The sample spans from 2013 to 2021. Each panel examines a measure of grid-level ship transit in terms of total distance in kilometers (km), total occupancy time in hours (hr), and the number of unique voyages or vessels transiting through the grid cell. Each column is a different sample: Global is the analysis using the whole sample. G. of Aden, G. of Guinea, and S.E. Asia restrict the sample to cells within each hotspot. Every panel-column combination is a different regression analysis. Encounters (3mo) is the count of pirate encounters recorded within the grid cell in the preceding 90 days. All specifications include Fixed-effects by Grid ID, ASAM Subregion, and ASAM region by year by month. Numbers in parentheses are Conley Standard Errors (100 km cutoff).

Table 2: Effect of Past Pirate Encounters on Shipping Voyages.

	Global	G. of Aden	G. of Guinea	S.E. Asia
<i>Panel (A): Total Distance (km)</i>				
Encounters (3 mo)	27.83*** (3.20)	210.90*** (19.58)	26.97*** (1.54)	22.43*** (3.50)
<i>Panel (B): Total Time (hr)</i>				
Encounters (3 mo)	2.25*** (0.33)	10.44*** (0.89)	1.96*** (0.14)	2.06*** (0.39)
<i>Panel (C): Average Speed (km/hr)</i>				
Encounters (3 mo)	-0.01* (0.01)	0.18*** (0.02)	0.04*** (0.01)	-0.02*** (0.01)
Observations	25,632,233	1,034,377	276,245	6,335,661
Hotspot FE	X	•	•	•

* $p < 0.1$, ** $p < 0.05$, *** $p < 0.01$ The unit of observation is a voyage. Each panel examines an observed feature in terms of total distance in kilometers (km), total time of the voyage in hours (hr), and the average speed of the voyage (km/hr). The sample spans from 2013 to 2021. Every column is a different sample: Global is the analysis using the whole sample. G. of Aden, S.E. Asia, and G. of Guinea restrict the sample to vessels passing through one of the hotspots, respectively. Every panel-column combination is a different regression analysis. Encounters (3mo) is the count of pirate encounters recorded in the projected path of the vessel in the preceding 90 days from the departure date using a 5 degree spatial footprint. Controls include average wind speed along the voyage and the wind-resistance index. Fixed effects include country-to-country combination, vessel type, vessel size, hotspot, and a battery of month by year and top port-to-port combination for country-to-country combination dummies.

125 construction decisions (see Supplementary Text S2.7.2).

126 **The private and public costs of modern-day piracy**

127 Having established robust empirical evidence about the statistical and directional impacts of
128 piracy encounters, we now consider their economic impact. Put simply, how much does the
129 avoidance behaviour of vessels cost in monetary terms? We answer this question by using
130 vessel characteristics to determine fuel and labor requirements along a given voyage, and then
131 empirically estimate changes in operational costs at the voyage level. The results are available
132 in Supplementary Text S2.4 and, consistent with our other findings, suggest that an additional
133 pirate encounter during the preceding three months translates to an average increase of US\$830
134 in input costs (comprising US\$580 in fuel and US\$260 in labor). While this estimate remains
135 largely consistent across data samples, again we observe a considerably larger effect in the Gulf
136 of Aden. Specifically, our estimates suggest that the marginal effect of a pirate encounter to
137 be over US\$5,000 in terms of fuel and over US\$1,000 in terms of labor. This discrepancy
138 is striking and it likely reflects the margins of adjustments that captains would pursue while
139 transiting different shipping routes.

140 We next explore how avoidance actions translate to emissions by establishing the link be-
141 tween pirate encounters and additional CO₂, NO_x and SO_x emissions by shipping vessels. The
142 regression results are provided in Supplementary Text S2.4. Overall, it follows that exces-
143 sive fuel consumption leads to concomitant emissions across the spectrum of related pollutants.
144 Specifically, we estimate that a single pirate encounter leads to an approximate increase of 4
145 tons of CO₂, 85 kg of NO_x, and 70 kg of SO_x per voyage, respectively. NO_x and SO_x excess
146 emissions are relatively less voluminous, though this is a direct consequence of their smaller
147 concentrations in bunker fuel relative to carbon. Once again, limiting the analysis to the Gulf
148 of Aden suggests impacts that are an order of magnitude larger.

149 To contextualize the practical significance of these estimates, we contrast the implied op-
150 erational and pollution costs of avoidance behaviour during our full 2013–2021 sample with a
151 counterfactual scenario that is absent any pirate activity at the global level. Figure 3 maps the
152 average annual costs to the shipping industry (fuel and labour costs), and additional emission
153 of air pollutants. To monetize these impacts, we use the social cost of each pollutant (11, 12)
154 and derive an aggregate measure of the global costs of piracy that averages US\$6.6 billion/year.
155 This figure corresponds to about 1.95% of the total private and public cost generated in by
156 the shipping sector in our sample. Approximately US\$1.5 billion of this topline number is at-
157 tributable to private operational (fuel and labor) costs, while US\$5.1 billion is attributable to
158 public damages (due to air pollution). ASAM regions 7 and 9 (containing the Southeast Asian
159 hotspot) account for US\$2.8 billion and US\$1.9 billion, ASAM region 6 (containing the Gulf
160 of Aden) accounts for US\$643 million, and ASAM region 5 (Gulf of Guinea) accounts for
161 US\$623 million. The results underlying Figure 3 are reported in detail in Supplementary Text
162 S2.5.

163 These results are intuitive. Adjustments by individual vessels may appear small, but the
164 relatively high density of shipping transit in places where pirate encounters occur makes the
165 total economic impact quite substantial, especially in terms of public damages.

166 **Discussion**

167 This paper has examined the effect of piracy on the shipping industry. We have documented
168 the mechanisms through which shippers adjust their behavior in response to reported pirate
169 encounters along a route, and the implied costs of shipping delays and environmental damages.
170 While our estimated adjustments may seem relatively small at the individual level, cumulatively
171 they translate to a significant economic welfare loss in the aggregate. Specifically, taking the
172 total flow of global shipping routes into account together with the prevalence of pirate attacks

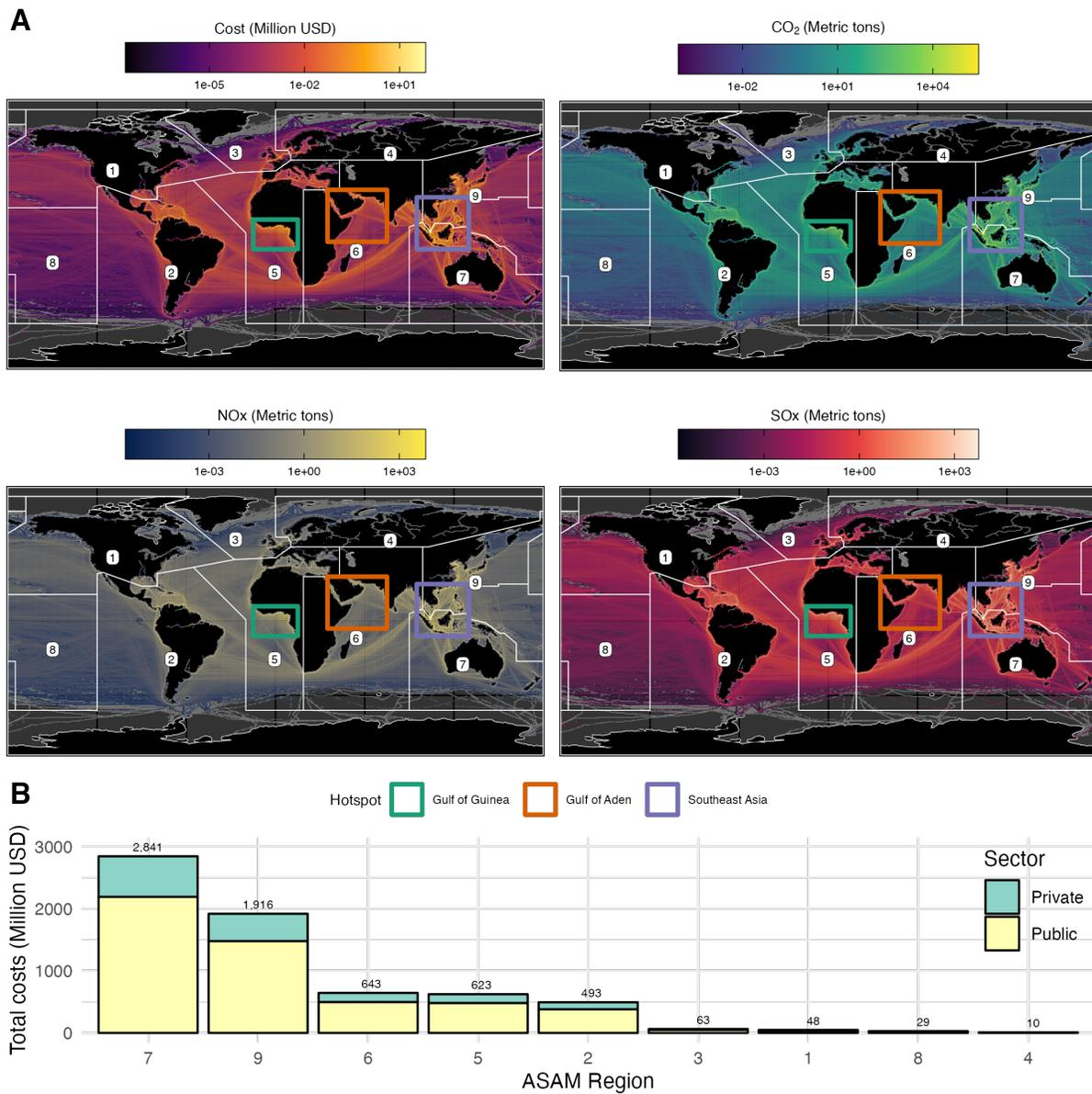


Fig 3: Additional Operational Costs and Emissions due to Piracy. Panel A shows maps of mean annual private costs to shippers (labor and fuel costs; Million USD), and additional CO₂, NO_x, and SO_x emissions (Metric tons). Note that data are log₁₀-transformed for visualization purposes and represented using a 0.5°x0.5° grid in geographic coordinates. Panel B shows the total costs (Million USD) associated with piracy by ASAM region, where we sum private costs to shippers as well as the cost of damages imposed by additional emissions based on the social-cost of each pollutant.

173 in some of the busiest shipping channels, we find that piracy avoidance is a considerable cost to
174 the shipping industry, as well as an overlooked source of environmental externalities.

175 The economic theory underlying our analysis suggests that ships will optimally adjust to
176 reduce the probability of pirate encounters. But those adjustments do not necessarily mean a
177 complete change of routes (i.e., start and end points remain the same). This intuition holds
178 up well in the data, where we observe ships traveling longer voyages, albeit at the cost of
179 higher fuel consumption and labor time. Each additional encounter amplifies this behavioural
180 response, and the effects have long-term implications after a single encounter is reported.

181 As we tried to emphasize, the Gulf of Aden is something of an anomaly in our empirical re-
182 sults, yielding effects that are up to an order of magnitude larger even than other piracy hotspots.
183 Why would the Gulf of Aden present such a different level of adjustment? This result could
184 be attributed to the prominence that Somali pirates and other armed assaults have occupied in
185 the public perception. But it could also reflect the geographical characteristics of the region,
186 which allows larger margins of adjustment for a given route. For example, vessels destined for
187 Europe can decide between going through the Gulf of Aden and crossing through Egypt, or cir-
188 cling around the Cape of Good Hope. All vessels going to Nigeria must go through the Gulf of
189 Guinea hotspot. As suggested by our theory, the way in which captains assess the relative piracy
190 risk of following a given path and the potential cost of doing so in different regions affects the
191 magnitude of their adaptation.

192 We note a few caveats. The first and most important to our causal identification, is the
193 assumption that prior pirate encounters occur at random, relative to the date of departure of
194 a given voyage. This assumption seems to hold in many instances, but some of the docu-
195 mented cases put the randomness assumption into question. In particular, hijacks that target
196 certain types of ships, or the possibility of encounters targeting one particular vessel or poorly-
197 enforced ports and anchorages. We control for all available observables, and use the nature of

198 shipping contracts to minimize the risk of presenting biased results. Given the robustness of our
199 results across a suite of model specifications (Supplementary Text S2.7) and the results from
200 an auxiliary instrumental variable analysis (Supplementary Text S2.6), we believe that we have
201 minimized the potential for these issues.

202 With these caveats in mind, we emphasize that the effect of piracy is clear and consistent
203 across the grid-level (reductions in measures) and voyage-level (increases in measures) por-
204 tions of the analysis. The consistency of the results highlights how problematic piracy is for the
205 shipping industry. But it also underscores the potential for piracy to have wider impacts that
206 ripple across the global economy. We can posit several channels through which these wider
207 impacts manifest. The first channel is a simple waste of capital. Because individual shippers
208 implement avoidance measures to reduce the probability of an encounter, they must allocate
209 capital to cover these actions. Such capital could have been used somewhere else, either in
210 the form of additional voyages, or as an input to other productive activities. A second channel
211 is environmental impacts. The adjustments to piracy are not emission-neutral. In the aggre-
212 gate, maritime commerce remains as one of the most emission-intense forms of transportation,
213 with direct contributions to both global greenhouse emissions and local air pollutants that may
214 disproportionately affect different areas and populations (13). Our calculations of additional
215 emission burdens shed some light on these potential effects, and highlight how piracy may
216 indirectly result in significant and harmful increases in emissions globally. A third channel
217 for wider economic impacts is the potential for indirect trade costs. Depending on the level
218 of competitiveness of the affected industry, and the routes in question, the associated costs in
219 transportation could simultaneously affect both producers and consumers. Previous studies have
220 tried to explore this problem using a trade framework (6, 7), and we believe that our approach of
221 examining individual voyages helps further clarify the mechanism behind trade effects, both at
222 a local and a global scale. Further investigation of this issue could unveil important implications

223 for developing legislation that ensures maritime security and fluid trade between nations.

224 Stepping back, three key insights derive from our results. First, the piracy problem remains
225 prevalent at a global scale. Second, because of the volume of voyages associated with the ship-
226 ping industry, individual avoidance behaviours accumulate into an economically meaningful
227 loss in aggregate welfare. These losses not only reflect the direct impact on trade flows and
228 transportation inputs (e.g., fuel costs), but also the indirect environmental costs from pollution.
229 Third, our results highlight the value of enforcement and anti-piracy measures for piracy-prone
230 areas. According to available public data (14), a cost-effective defense task could be deployed
231 for roughly \$330M/year (adjusted for inflation). Enforcement spending would thus cost only a
232 fraction of the total value currently lost due to piracy, and could help reduce large private and
233 public costs (14). Addressing this missing enforcement will require active cooperation from
234 multiple sectors and nations. The benefits, however, can be enjoyed widely.

235 Finally, an important angle of this issue relates to tackling the roots of the piracy problem
236 in the developing world: poverty. Partnerships involving both public and private participation
237 could potentially prove highly cost-effective and generate benefits at a large scale. Studying the
238 design and implementation of such policies is a promising area for future research.

239 **References and Notes**

- 240 1. R. Asariotis, *et al.*, Review of maritime transport, 2017, *Tech. rep.*, United Nations Confer-
241 ence on Trade and Development (2017).
- 242 2. P. Gosse, *The history of piracy* (Courier Corporation, 2012).
- 243 3. J. L. Anderson, *Journal of World History* pp. 175–199 (1995).
- 244 4. J. Bahadur, *The pirates of Somalia: Inside their hidden world* (Vintage, 2011).

- 245 5. C. Bueger, *Third World Quarterly* **34**, 1811 (2013).
- 246 6. A. Burlando, A. D. Cristea, L. M. Lee, *Review of International Economics* **23**, 525 (2015).
- 247 7. S. Bensassi, I. Martínez-Zarzoso, *Review of International Economics* **20**, 869 (2012).
- 248 8. P. Hallwood, T. J. Miceli, *Scottish Journal of Political Economy* **60**, 343 (2013).
- 249 9. D. A. Kroodsma, *et al.*, *Science* **359**, 904 (2018).
- 250 10. S. Wang, Q. Meng, *Transportation Research Part E: Logistics and Transportation Review*
251 **48**, 701 (2012).
- 252 11. Interagency Working Group on Social Cost of Greenhouse Gases [United States Govern-
253 ment], Technical support document: Social cost of carbon, methane, and nitrous oxide
254 interim estimates under executive order 13990, Online (2021).
- 255 12. M. Mier, J. Adelowo, C. Weissbart, Taxation of carbon emissions and local air pollution in
256 intertemporal optimization frameworks with social and private discount rates (2021).
- 257 13. J. J. Corbett, P. Fischbeck, *Science* **278**, 823 (1997).
- 258 14. D. C. Sonnenberg, Maritime law enforcement a critical capability for the navy, Ph.D. thesis,
259 Monterey, California. Naval Postgraduate School (2012).
- 260 15. D. J. McCauley, *et al.*, *Science* **351**, 1148 (2016).
- 261 16. G. F. Watch, Anchorages, ports and voyages data (2021).
- 262 17. S. Betz, Reducing the risk of vessel strikes to endangered whales in the santa barbara chan-
263 nel, Ph.D. thesis, University of California, Santa Barbara (2011).

- 264 18. J. J. Corbett, H. Wang, J. J. Winebrake, *Transportation Research Part D: Transport and*
265 *Environment* **14**, 593 (2009).
- 266 19. C. Wang, J. J. Corbett, J. Firestone, *Environmental science & technology* **41**, 3226
267 (2007).
- 268 20. M. Ester, H.-P. Kriegel, J. Sander, X. Xu, *et al.*, *Kdd* (1996), vol. 96, pp. 226–231.
- 269 21. T. G. Conley, *Journal of econometrics* **92**, 1 (1999).
- 270 22. A. P. Rubin, *Int'l L. Stud. Ser. US Naval War Col.* **63**, 13 (1988).
- 271 23. T. Gray, *Reports of the Transactions of the Devonshire Association for the Advancement of*
272 *Science* **121**, 161 (1989).
- 273 24. G. V. Scammell, *Modern Asian Studies* **26**, 641 (1992).
- 274 25. K. R. Andrews, *The Spanish Caribbean: trade and plunder, 1530-1630* (Yale University
275 Press New Haven, 1978).
- 276 26. J. F. Warren, *The Sulu Zone, 1768-1898: The dynamics of external trade, slavery, and*
277 *ethnicity in the transformation of a Southeast Asian maritime state* (NUS Press, 2007).
- 278 27. A. Tenenti, *Piracy and the Decline of Venice, 1580-1615* (Univ of California Press, 1967).
- 279 28. R. Wright, *Financial Times*, November **20** (2008).
- 280 29. A. Bowden, K. Hurlburt, E. Aloyo, C. Marts, A. Lee, *The economic costs of maritime*
281 *piracy* (One Earth Future Foundation, 2010).
- 282 30. R. J. O'Connell, C. M. Descovich, Decreasing variance in response time to singular inci-
283 dents of piracy in the horn of africa area of operation, *Tech. rep.*, Naval Postgraduate School
284 Monterey CA Department of Information Sciences (2010).

- 285 31. B. Guha, A. S. Guha, *Economics letters* **111**, 147 (2011).
- 286 32. C. Liss, *Private Military and Security Companies* (Springer, 2007), pp. 135–148.
- 287 33. M. Flückiger, M. Ludwig, *Journal of Development Economics* **114**, 107 (2015).
- 288 34. S. Axbard, *American Economic Journal: Applied Economics* **8**, 154 (2016).
- 289 35. P. T. Leeson, *Journal of political economy* **115**, 1049 (2007).
- 290 36. G. A. Psarros, A. F. Christiansen, R. Skjong, G. Gravir, *Journal of transportation security*
291 **4**, 309 (2011).
- 292 37. J. Bahadur, *US Naval Institute Proceedings* (2011), vol. 137, pp. 73–74.
- 293 38. ICC-IMB, Piracy and armed robbery against ships: Report for the period 1 january - 31
294 december 2017, *Tech. rep.*, International Maritime Bureau of the International Chamber of
295 Commerce (2018).
- 296 39. J. Jansson, *Liner shipping economics* (Springer Science & Business Media, 2012).
- 297 40. M. Stopford, *Maritime economics* (Routledge, 2013).
- 298 41. S. R. Massel, *Ocean surface waves: their physics and prediction*, vol. 36 (World scientific,
299 2013).

300 **Acknowledgements**

301 We thank Christopher Costello, Anca Cristea, Javier Birchenall, Kyle Meng, Olivier Desch-
302 enes, Owen Liu, and Christopher Severen for helpful comments on the paper. We also acknowl-
303 edge valuable feedback from participants at the Econometrics Lunch and the Environmental

304 Lunch at the University of California at Santa Barbara (UCSB), the Workshop in Environmen-
305 tal Economics and Data Science at the University of Oregon, and the Summer Conference of
306 the Association of Environmental and Resource Economics. We thank Global Fishing Watch
307 for providing the data processing and data management infrastructure for the shipping data. We
308 would also like to thank Google for providing in-kind computational support.

309 **Funding**

310 Partial funding for this project was provided by the Research Provost Award at the University of
311 Miami, the Latin American Fisheries Fellowship at the University of California Santa Barbara,
312 the Chilean Government through the Becas Chile program, and the Environmental Markets
313 Laboratory at the University of California, Santa Barbara.

314 **Author Contribution**

315 Conceptualization was performed by R.M, J.C.V.D., G.McDo., and G.McDe. Data curation
316 was performed by R.M, J.C.V.D., and G.McDo. Formal Analysis was performed by R.M
317 and J.C.V.D. Funding acquisition was performed by R.M. Investigation was performed by
318 R.M, J.C.V.D., and G.McDo. Methodology was performed by R.M, J.C.V.D., G.McDo., and
319 G.McDe. Project administration was performed by R.M. Supervision was performed by R.M.
320 Validation was performed by R.M, J.C.V.D., G.McDo., and G.McDe. Visualization was per-
321 formed by J.C.V.D. and G.McDo. Writing – original draft was conducted by by R.M, J.C.V.D.,
322 G.McDo. Writing – review & editing was performed by R.M, J.C.V.D., G.McDo., and G.McDe.

323 **Competing interests**

324 The authors declare no competing interests.

325 **Data and materials availability**

326 All data and materials will be available at [https://github.com/renatomolinah/](https://github.com/renatomolinah/piracy-shipping)
327 piracy-shipping

328 **Supplementary Materials**

- 329 • Materials and Methods
- 330 • Supplementary Text
- 331 • Figs. S1 to S11
- 332 • Tables S1 to S23
- 333 • References 15 to 41

334

Supplementary Materials for:

335

***Dangerous Waters: The Economic Toll of Piracy on Maritime
Shipping***

336

337

Renato Molina, Juan Carlos Villaseñor-Derbez,

338

Gavin McDonald & Grant McDermott

S1 Materials and Methods

S1.1 Data

We construct a unique dataset for global shipping and piracy that provides both temporal and spatial variation. Specifically, we compile a panel dataset from 2013 to 2021 that includes individual shipping voyages and recent anti-shipping encounters along the route of each voyage. The panel includes the most important operational components that determine the cost of shipping voyages (e.g., engine size, number of crew members, route taken) as well as environmental factors affecting it (e.g., wind speed and direction).

S1.1.1 Shipping activity

Individual shipping vessel voyage-tracks come from the Automatic Identification System (AIS) satellite latitude and longitude data. AIS transponders are required on all vessels greater than 300 gross registered tons while operating on international voyages, and by many countries while operating in certain exclusive economic zones (15). The dataset from 2013-2021 includes over 100,000 unique known cargo, tanker, and reefer vessels as defined by vessel identification data provided by Global Fishing Watch (GFW) (9). We include vessels that are classified by GFW as one of *cargo*, *cargo* or *tanker*, *bunker* or *tanker*, *tanker*, *cargo* or *reefer*, *specialized reefer*, *container reefer*, *reefer*, or *bunker*. These vessels broadcast more than 10 billion individual AIS messages during our study period, which we assigned to more than 26 million individual voyages. We leverage GFW's datasets of ports and voyages in order to assign every single AIS message to a specific port-to-port voyage by a specific vessel (16).

Data on operational costs come from two sources: fuel consumption and labor. We calculate fuel consumption using main engine power, gross tonnage, auxiliary engine power, and design speed. Main engine power and gross tonnage come from the Global Fishing Watch vessel characteristics database (9). For each vessel, we determine these characteristics using a hierarchy based on data availability: 1) the official registered information of the vessel; and 2) values inferred by the Global Fishing Watch vessel characteristic neural network when available. Auxiliary power is a function of main engine power, and is calculated using known empirical relationships (17), which link main propulsory requirements with vessel characteristics and auxiliary needs. Design speed is a function of main engine power and gross tonnage (17).

Using these vessel characteristics, we calculate fuel consumption using a standard approach that combines fuel consumed by both the main and auxiliary engines (18). Fuel consumption of the main engine is defined by hours of operation, main engine power, main engine specific fuel consumption rates (19), and a cubic law of operational speed relative to design speed. Fuel consumption of the auxiliary engine is defined by operating hours, auxiliary engine power, and auxiliary engine specific fuel consumption rates (19). Fuel consumption was calculated for each individual AIS ping which were then summed for each voyage.

Daily fuel price data come from Bunker Index. We use the 380 CST Bunker Index, which is the global average price from all ports selling 380 centistoke fuel, the most commonly used fuel

377 in maritime transport. For dates with missing price data, we impute the missing value using the
378 most recent reported price. Most gaps in the data do not exceed more than two days. Total fuel
379 cost for each voyage is then calculated by multiplying the total fuel consumption of the voyage
380 by the fuel price on the date of departure.

381 We also keep track of labor requirements for individual voyages. Using the ratio suggested
382 in the literature (17), we estimate the crew needed to operate a vessel as a function of its size and
383 type. The crew wage is calculated using the 2018 International Transport Worker’s Federation
384 wage scale for the average non-officer seafarer.⁴

385 We also calculate emissions of CO₂, NO_x, and SO_x for each voyage. CO₂ emissions are
386 calculated using a linear relationship (18), which relies on total fuel consumption of the voyage.
387 SO_x emissions are calculated similarly, under the assumption of 3.3% sulfur content for each
388 kilogram of fuel (13). Similarly, NO_x emissions are calculated using a separate conversion rate
389 for both the main engine fuel consumption (which we assume to be a slow-speed engine) and
390 auxiliary engine (which we assume to be a medium-speed engine) (13).

391 Finally, we incorporate a weather proxy in the form of average wind speed and direction
392 along each voyage. We call this proxy the wind-resistance index. Wind data come from the
393 NOAA Global Forecast System Atmospheric Model. Mean monthly wind speed and direction
394 information is calculated for 5°x5° grid cells. We take into account wind direction by decom-
395 posing the pitch angle relative to the vessel; the resistance is concave or convex depending on
396 the vessel going against, or with the wind. This measurement is symmetric in absolute terms
397 along each 90° portion of a full circumference and it goes from 0 to 1. Scaling this measurement
398 by the wind speed gives the final wind-resistance index. For each voyage, the time-weighted
399 mean wind-resistance is then calculated based on the voyage’s time spent in each 5°x5° cell.

400 The final panel covers all global valid cargo and tanker voyages between 2013 and 2021,
401 with each entry reporting vessel characteristics (type, size, crew), departure and arrival dates,
402 departure and arrival ports and countries, total distance traveled (km), time traveled (hr), speed
403 (km/hr), fuel consumption (kg), fuel and labor cost (US\$), and emissions (kg).

404 **S1.1.2 Pirate encounters**

405 We operationalize pirate encounters by using the anti-shipping data provided by the United
406 States National Geospatial Intelligence Agency, which includes dates and locations of sightings
407 and hostile acts against ships by pirates, robbers, and other aggressors. We include all anti-
408 shipping encounters in our dataset except those categorized as “Suspicious Approach,” as those
409 are not confirmed.⁵ We then divide the ocean into two global grids: one of 0.5° latitude by 0.5°
410 longitude pixels and one of 5° latitude by 5° longitude pixels. We use the 0.5°x0.5° data for a
411 fine-scale pixel-level analysis, and use the 5°x5° data for a port-to-port voyage-level analysis.⁶

⁴Current and projected wages are available at <https://t.ly/JADDs> [Last Visited on 04/12/24]

⁵This dataset is available at: <https://t.ly/jbmqG> [Last Visited on 04/12/24]

⁶At the equator, a cell of 5° by 5° is roughly equivalent 345 by 345 miles, which is a reasonable spatial area over which shipping vessel operators might make route and speed adjustment decisions in relation to recent anti-

412 For each gridded dataset, we then calculate the number of anti-shipping encounters that occurred
413 in each pixel on each day. For any given pixel and any given day of shipping operation in that
414 pixel, this therefore allows us to calculate the number of days since the most recent encounter
415 in that pixel, as well as the number of encounters that occurred within that pixel over a rolling
416 time window. For the pixel-level analysis, we calculate the number of encounters within three
417 different rolling window of the past 3, 6, and 12 months for every $0.5^\circ \times 0.5^\circ$ pixel and every day
418 in the dataset.

419 For the voyage-level analysis, we first calculate the number of encounters within the $5^\circ \times 5^\circ$
420 pixels along each port-to-port voyage that occurred within a rolling window of the past 3
421 months. This provides the number of recent pirate encounters in the area that each voyage
422 passes through. This represents, for any given voyage departure date for any given port-to-port
423 route, the captain's expectation of how many encounters they might expect could occur along
424 the route they are about to embark on.

425 Using the locations of individual anti-shipping encounters that occurred from 2010 through
426 2021, we also determine hotspots of encounters using density-based clustering as described
427 by (20). Implementing a cluster reachability distance of 10 km, and a minimum number of
428 encounters per cluster of 300, we find that attacks correspond to three hotspots of intensive
429 pirate activity for the entire panel: the Gulf of Aden, the Gulf of Guinea, and Southeast Asia.
430 For each of these hotspots we generate a rectangular bounding box that is snapped to the nearest
431 5° latitude and 5° longitude markers that fully enclose each set of hotspot attacks, and then for
432 each voyage we then determine whether the vessel transited through one or more of these areas.

433 The final overlap between shipping voyages and pirate encounters, which is the dataset used
434 in the empirical analysis, is shown in Figure 1. Note that pirate encounters concentrate in a few
435 areas in the map. Particularly in the Caribbean, the Gulf of Guinea, the coast of East Africa,
436 the Arabian Sea, and the jurisdictional waters of the Philippines and Malaysia. The relevant
437 hotspots for this study are enclosed by the rectangles.

438 **S1.2 Empirical analysis**

439 **S1.2.1 Grid-level analysis**

440 To establish the effect of piracy on shipping we will rely on several estimation procedures. First,
441 we begin by generally asking if shipping transit is apparently affected by pirate encounters. The
442 analysis is performed under an Eulerian framework, with the units of analysis as grid cells along
443 a $0.5^\circ \times 0.5^\circ$ grid. In particular, we are interested in how measures of shipping traffic (i.e., total
444 distance traveled within a grid cell or total time spent by ships in a grid cell, number of voyages
445 and vessels crossing a grid cell) change following a pirate encounter. Summary statistics for
446 this dataset are provided in Table S1.

We extend this analysis with a fixed-effect regression approach connecting pirate encounters
shipping encounters. Moving at 10 knots, this is an area that potential attackers could cover in just 30 hours.

and shipping traffic within grid cell i at time t . The model takes the following form:

$$y_{it} = \beta TNE_{it} + \gamma' G_i + \theta' X_t + \eta_i + \epsilon_i \quad (\text{S1})$$

447 y is the response variable, and TNE is the total number of encounters during the past three
 448 months, relative to date t . β is the average marginal change related to an additional encounter
 449 on mean traffic over a cell. $\gamma' G_i$ is a vector of fixed effects for the subregion used by the Anti-
 450 shipping Activity Messages (ASAM subregion), $\theta' X_t$ captures temporal fixed effects by ASAM
 451 region-year-month, while η_i correspond to grid-specific fixed effects. We estimate spatial HAC
 452 standard errors with a 100 km cutoff (21). This analysis restricts the sample to grids with at
 453 least one attack during our analysis window (2013-2021; $N = 590$ cells). The identification
 454 assumption is that the timing and location of past encounters are exogenous to a voyage after
 455 controlling for temporal and grid-specific fixed effects.

456 In addition, we estimate dynamic treatment effects by regressing ship traffic on dummy
 457 variables indicating relative time (days) to treatment. We include the same battery of fixed
 458 effects as in the aggregate effect approach. This ancillary analysis retains only cells that have
 459 at least five days without other encounters before and after the focal encounter date ($N = 233$
 460 cells).

461 S1.2.2 Voyage-level analysis

We then analyze the effect of piracy at the voyage level. We are interested in the feature of a given voyage i (i.e., distance, duration, and speed) along country-to-country route, r , at time t , and their associated consequences in terms of operational costs and emissions. The model is as follows:

$$y_{irt} = \alpha + \beta TNE_{rt} + \delta_i VC_i + \lambda_i W_i + \eta_r R_i + \theta' X_t + \epsilon_{irt} \quad (\text{S2})$$

462 y is the response variable, and TNE is the total number of encounters during the last three
 463 months, with β as the average marginal effect of an additional encounter on the mean path of a
 464 voyage. VC is a vector of fixed effects according to vessel characteristics (i.e., type of vessel
 465 and size), while W is the time-weighted mean wind-resistance index and average wind speed
 466 for a given voyage. Finally, R is a vector of fixed effects by route, while X_t is a battery of month
 467 by year fixed effects. In the results we will also specifically control for additional factors such
 468 as crossing hotspots or the voyage being part of the most common port-to-port combination
 469 between countries. To account for potential route and temporal correlation, we cluster standard
 470 errors by country-to-country route by year. The identification assumption is that the timing and
 471 location of past encounters are exogenous to the date of departure of a given vessel.

472 S2 Supplementary Text

473 S2.1 Background

474 S2.1.1 Piracy and trade

475 Modern piracy is fundamentally an enforcement problem that can be traced to poorly defined
476 property rights and duties over maritime territory. This misalignment is especially acute in in-
477 ternational settings, where the establishment and enforcement of anti-pirate regulations usually
478 conflicts with sovereign rights (22). These institutional settings reduce the probability of pi-
479 rates being prosecuted, or even apprehended, which in equilibrium encourages the continued
480 predation of sea commerce.

481 From a welfare perspective, Anderson suggests several types of losses associated with
482 piracy (3). First, the direct capital losses to violence, which manifest either in the form of
483 damages to the ship or cargo, or as the loss of life. Second, the indirect losses in the form of
484 resources channeled toward evasion and protection that could have been used for other produc-
485 tive activities. For example, the additional bulk of fuel used to maintain evasive maneuvers, or
486 the additional amount of capital required to sustain a steady flow of goods *vis-à-vis* the same
487 exchanges in the absence of piracy. It follows that the magnitude of these responses can lead
488 to both intensive and extensive margin adjustments, which in turn can cause dynamic losses
489 in the form of diminished incentives for producers and merchants to continue with or expand
490 production (3).

491 Historical data suggest that piracy events have often been followed by extremely negative
492 impacts to commerce channels and local economies. For example, during the seventeenth cen-
493 tury, the “Turkish pirates” completely paralyzed several parts of west England (23). During
494 the same period, the predominance of pirate organizations in the Arabian sea also led to se-
495 vere decreases in trade flow, with devastating consequences for all industries in the region (24).
496 These two cases are not unique. Similar links have been documented for other trade regions in
497 the Caribbean (25), the Philippines (26), and Venice (27). All of these examples illustrate how
498 thriving economies suffer considerable negative effects due to piracy.

499 Modern piracy has had similar effects. In fact, piracy remains a problem worldwide. There
500 were over 2,200 pirate and anti-shipping encounters globally between 2013-2021, with over
501 600 taking place between 2019-2021. Most encounters, however, take place in a few hotspots;
502 namely: the Gulf of Aden (known for the Somali pirates), the Gulf of Guinea (mostly within
503 the Nigerian EEZ), the Malacca Straits (the shipping channel formed by Sumatra and the Malay
504 peninsula) and the South China sea. For the remainder of the paper we will refer to both
505 the Malacca Straits and the South China sea as one group that we call Southeast Asia. The
506 distribution of the actual number of encounters in each region over time is shown in Figure 1.
507 From this figure, note that pirate encounters are consistently concentrated in the African region
508 and Southeast Asia.

509 Although sparse, there are several assessments regarding the economic impact of modern
510 piracy. Past estimates suggest that the losses in trade volume due to pirate activities in Somalia

511 accrued to about \$24 billion/year (6). Other estimates are more conservative and suggest that
512 the loss ranged between \$1 billion and \$16 billion, when accounting for the addition of 20
513 days per voyage due to re-routing around Africa, and increased insurance, charter rates, and
514 inventory costs (28–30). Another study estimates that 10 additional hijacks in either the Gulf of
515 Aden or the Strait of Malacca reduce the volume of exports between Asia and Europe by about
516 11%, with an estimated cost of about \$25 billion per year (7). These studies estimate losses
517 through the examination of overall trade patterns, but to the best of our knowledge, there is no
518 study focusing on the behavior of individual shipping vessels. We believe the latter is a more
519 direct way to disentangle the cost of piracy. It is plausible that the gap in the literature regarding
520 the effect of piracy on shipping patterns is due to the difficulty of obtaining data on individual
521 shipping voyages, but also because of the sparse data on pirate activities. Both of these issues
522 are accounted for in this paper.

523 On the other hand, theoretical insights regarding the piracy problem can be traced to two
524 studies. Namely, Guha and Guha (31), who model optimal patrolling and penalties under the
525 option of self insurance, and Hallwood and Miceli (8), who explore optimal patrolling and
526 penalties taking into account strategic interactions between pirates and shippers. Although very
527 valuable contributions in terms of formalizing the theory behind pirate behavior, neither paper
528 explored vessel adjustments along shipping routes as they focus on penalties and enforcement.

529 Other related literature has devoted efforts to several topics on both past and modern piracy.
530 One of those topics relate to anti-piracy efforts. Anderson (3) documents the historical evo-
531 lution of state and individual actions to control for piracy along shipping routes. Similarly,
532 Liss (32) describes how modern piracy incentivizes shippers to employ private military com-
533 panies or acquire their own defense mechanisms. Other empirical settings, including Flückiger
534 and Ludwig (33), as well as Axbard (34), study how poor fishing conditions lead to an increase
535 in pirate activity in Africa and Indonesia, respectively.

536 Finally, other authors such as Leeson (35) and Psarros, Christiansen, and Skjong (36) study
537 the factors that contribute to pirates being more or less effective in terms of finding vessels, as
538 well as extracting the most value out of these encounters. In addition and specific to the Somali
539 case, references O’Connell and Descovich (30), as well as Bahadur (37) document the social
540 and economic institutions associated with pirate activities by identifying ransom procedures,
541 operational supply chains, and community support.

542 **S2.1.2 The business model of modern piracy**

543 Establishing how pirate operate globally presents several challenges. First, pirates often have
544 little or no incentive to make the details of their operations known to the public. Nonetheless,
545 there are still a few credible sources that allow us to establish the mechanics behind pirate en-
546 counters, and more importantly, use them as means for identification in the empirical section. In
547 particular, we make use the information documented by Bahadur (4), which relies on a number
548 of interviews with individuals who claimed to be associated, directly or indirectly, with pirates
549 in Somalia in 2009. Considering the sensitivity of the piracy issue, these interviews provide the

550 best available information on the actual behavior and incentives of pirates.

551 Pirates in Somalia appear to not discriminate between vessels. Instead they opportunis-
552 tically hijack vulnerable vessels that cross their path. Once the potential target is identified,
553 pirates pursue the vessel until eventually capturing it, or the vessel is realistically out of reach.
554 Neither the search or the pursuit are constrained by the jurisdictional boundaries of Somalia.
555 The boarding strategy entails the pirate crew splitting into several skiffs, which approach the
556 target vessel from all sides while waving and firing their weapons to scare the ship's crew. If the
557 vessel stops, or the skiffs are able to keep up with it, the pirates would toss rope ladders onto
558 the deck and then proceed to boarding. According to the accounts, crews rarely resist boarding
559 once the pirates successfully get on the deck. The average reported success rate of the pirates
560 used to be about 20 to 30% (4).

561 Once the pirates successfully take control of the ship, they steer the vessel to a friendly
562 port. At this location, an additional set of guards and translators would board the ship, and
563 ransom negotiations will start. Most ransoms would be handled by insurance companies. Upon
564 reaching an agreement, the money is usually delivered via parachute drop-off onto the deck of
565 the ship, and then split amongst the pirates. The amount that each of them would receive is a
566 fixed fraction of the total ransom, and it would vary depending on the task (4). About half of
567 the pot would go to the actual men boarding the ship, one third to the investors financing the
568 operation, and a sixth to everyone else assisting with logistics and enforcement.

569 We note that although 2017 saw a spike in pirate activities in the Gulf of Aden, this region
570 seems to be no longer affected at same scale as it used to be during the 2000's.⁷ According
571 to the latest reports on encounters by the US government (Figure 1B) and the International
572 Maritime Bureau of the International Chamber of Commerce (ICC-IMB), most encounters are
573 now reported to take place in the Gulf of Guinea and Southeast Asia (38). The business model
574 of piracy in these regions, however, differs from the Somali pirates.

575 Pirates in the Gulf of Guinea follow a similar approach when it comes to intercepting a ves-
576 sel. The difference comes after they have successfully hijacked the ship. Specifically, besides
577 hijacking the vessel and its crew, these pirates appear to focus on kidnapping only a subset of
578 crew members for ransom (38). Another regular practice in this region is the robbery of cargo,
579 especially liquid fuel.⁸

580 Pirate encounters in Southeast Asia seem to follow a variation of the previous business
581 model. According to recent reports, and in addition to the practices listed above, encounters
582 include large-scale and sophisticated operations targeted at siphoning fuel from tanker vessels.⁹
583 In this type of attack, vessels are also approached and hijacked, but then they are steered towards
584 a siphoning facility on the shore that retrieves the entire cargo. Under this model, the crew and

⁷See for example *Piracy threat returns to African waters* by CNN, available at: <https://t.ly/qKlZo>
[Last Visited on 04/12/24]

⁸See *Abduction of Crew Off Nigeria Brings Piracy Back to Indian Agenda* by The Wire, available at: <https://t.ly/gVvXJ> [Last Visited on 04/12/24]

⁹See *Pirates in Southeast Asia: The World's Most Dangerous Waters* by Time, available at: <https://t.ly/Ano8q> [Last Visited on 04/12/24]

585 the ship are usually freed several days after a successful attack (38).

586 Finally, pirate encounters have also increased in the Caribbean, especially along the coast
587 of Venezuela. Their approach, however, seems to be fundamentally different. Recent reports
588 indicate that due to harsh economic conditions in Venezuela and northern Colombia, many of
589 the coast inhabitants target private yachts for small robbery.¹⁰ These encounters are suggested
590 to be sporadic, and usually deriving in opportunistic predation of groceries and other valuable
591 items that tourists carry. To our knowledge, no hijacks or ransoms for cargo vessels have been
592 reported in this region.

¹⁰See *La piratería regresa al Caribe motivado a la crisis de Venezuela* by El Nacional, available at <https://t.ly/ug40>– [Last Visited 04/12/24]

593 **S2.2 An economic model of pirates and shippers**

594 This section establishes the intuition behind shipping behavior in the face of piracy. In particu-
 595 lar, we illustrate the mechanisms behind pirate encounters, and their effect on shipping routes.
 596 It follows that all relevant costs associated with piracy can be attributed to deviations from
 597 cost-effective behavior in the absence of the threat. The model we propose builds on the previ-
 598 ous efforts (8, 31), who championed the theoretical understanding of piracy under an economic
 599 framework.

600 For simplicity, assume a situation where there is only one pirate and one shipper. There is
 601 a continuum of paths, $x \in \mathbb{X} = [0, \bar{x}]$, for a certain route. The cost-effective path is given by
 602 $x = 0$, while $x = \bar{x}$ represents the most expensive, but feasible, path. One way to think about
 603 this idea would be vessels having to sail farther from the coast than optimal due to the threat of
 604 piracy. The cost of deviating from the optimal path, $c(x)$, is strictly convex in x , and $c(0) = 0$.
 605 In the presence of piracy, the shipper chooses the route taking into account the possibility of
 606 encountering and being attacked by the pirate.

607 An encounter might occur when the shipper transits through the area monitored by the
 608 pirate, which is given by the segment $x : x \in [0, \bar{a})$. Because physical limitations prevent
 609 pirates from monitoring all possible transportation paths, it follows that $\bar{a} < \bar{x}$. The probability
 610 of an encounter, however, is strictly positive along the $[0, \bar{a})$ interval, and zero everywhere
 611 else. One way to think about this feature is the shipper taking an extremely long path with no
 612 risk of piracy, or using other transportation methods such a trains or airplanes. Formally, this
 613 relationship can be expressed as:

$$\phi(x; \theta) \begin{cases} > 0 & ; \quad 0 \leq x < \bar{a} \\ = 0 & ; \quad \text{Otherwise} \end{cases} \quad (\text{S3})$$

614 with θ being the vector of parameters that characterize the distribution, including \bar{a} and the
 615 search effort with which pirates patrol the susceptible waters. The probability function satisfies
 616 $\phi_x(x, \theta) < 0$ and $\phi_{xx}(x, \theta) > 0 \forall x \in [0, \bar{a})$, and $\phi_x(x, \theta) = \phi_{xx}(x, \theta) = 0 \forall x \in [\bar{a}, \bar{x}]$.

617 In this model, the pirate decides to attack only after an encounter takes place, in which the
 618 shipper loses h . From the pirate's perspective, however, the assault can be either successful
 619 (the pirate gets away) or unsuccessful (the pirate gets caught). An attack implies the pirate
 620 obtaining a monetary prize or booty, b , which is not necessarily equal to h , and that he cannot
 621 determine until the encounter occurs. This assumption implies that the pirate treats b as a
 622 randomly distributed variable with cumulative distribution $F(b)$ over support $[0, \bar{b}]$. One way to
 623 think about this realization is the assessment of the ship being "worth" pursuing (4).

624 Before attacking, the pirate assesses the monetary value of the booty with the expected
 625 costs of being apprehended with probability, p , and fine, f . As the pirate does not serve time
 626 incarcerated,¹¹ it follows that an attack occurs whenever $b \geq pf$. Therefore, conditional on an

¹¹Reference (31) notes that a major problem in modern piracy is the lack of credible punishment after aggressors have been apprehended.

627 encounter, the probability of an attack is given by:

$$\psi(pf) = [1 - F(pf)] \quad (\text{S4})$$

628 Finally, the model assumes the shipper cannot observe the patrolling effort of the pirate, but
 629 a finite number of paths previously taken for the origin-destiny combination. Denote this history
 630 set as $\mathbf{z} = \{z_1, \dots, z_m\}$ for m different voyages. The shipper also knows which paths have expe-
 631 rienced encounters in the past (e.g., through access to the monthly *Worldwide Threat to Shipping*
 632 reports published by the Office of Naval Intelligence, or by contracting intelligence firms that
 633 provide such information). This complimentary history set is given by $\mathbf{y} = \{y_1, \dots, y_n\}$, for
 634 a total of n encounters. With this information, the shipper can estimate the parameters of the
 635 encounter probability distribution, including the span of the monitored area, as:

$$\hat{\theta} = \arg \max_{\theta} \{\mathcal{L}(\theta; \mathbf{y}, \mathbf{z})\} \quad (\text{S5})$$

636 with $\mathcal{L}(\theta; \mathbf{y}, \mathbf{z})$ as the likelihood function of $\phi(x, \theta)$. If the market price of the voyage is given
 637 by π , it follows that the expected net return for the shipper, R , would be finally given by:

$$R(\pi, x, \hat{\theta}) = \pi - \phi(x, \hat{\theta})\psi(pf)h - c(x) \quad (\text{S6})$$

638 Assuming risk neutrality, the shipper's problem can be solved using standard optimization
 639 techniques, and it follows that the optimal path is characterized by the proposition below:

Proposition 1. *The optimal path for a shipper in the face of piracy, x^* , depends on the information of past voyages and pirate encounters, $\{\mathbf{y}, \mathbf{z}\}$, and it satisfies:*

$$-\phi_x(x^*, \hat{\theta})\psi(pf)h = c'(x^*) \quad (\text{S7})$$

640 with

$$\hat{\theta} = \arg \max_{\theta} \{\mathcal{L}(\theta; \mathbf{y}, \mathbf{z})\} \quad (\text{S8})$$

641 *All proofs are provided in Supplementary Text S2.2.2.*

642 Proposition 1 indicates that the optimal path equalizes marginal expected savings to the
 643 marginal cost of deviating from the cost-effective one. The set of feasible optimal paths is then
 644 given by the Lemma below:

645 **Lemma 1.** *The optimal path for a shipper in the face of piracy is contained in the set $x : x \in$
 646 $(0, \bar{a}]$.*

647 Lemma 1 suggests two points regarding optimal paths. First, the shipper will never ignore
 648 the threat of piracy. Expected losses from encountering and being attacked by a pirate will
 649 always be taken into account and thus avoided following the equimarginal principle. Second and
 650 consistent with cost minimizing behavior, if the cost of deviating is low enough, total avoidance

651 will never exceed \bar{a} . These ideas are illustrated in figure S1, with panel (a) corresponding to
 652 interior solutions and panel (b) corresponding total, or maximum, avoidance.

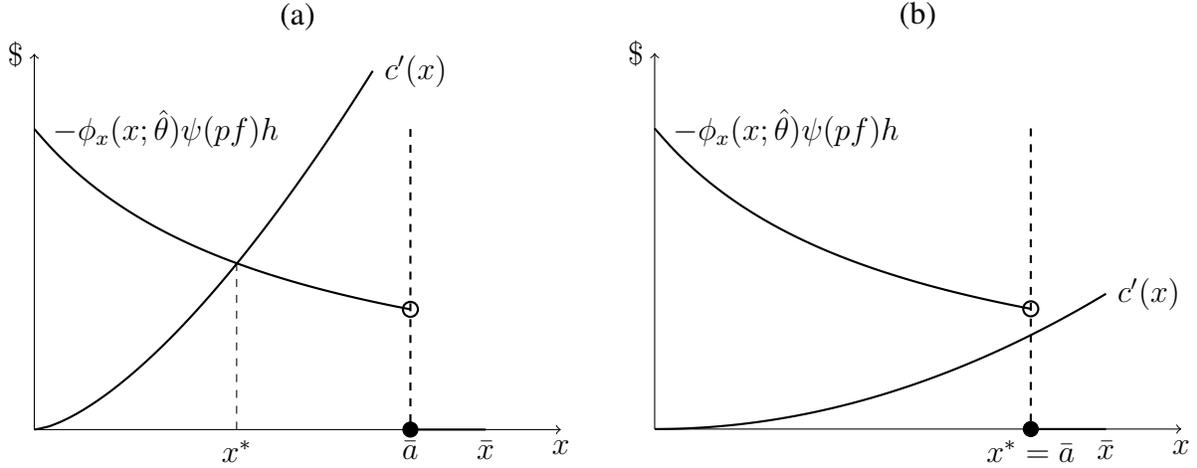


fig S1: **The shipper's path selection problem.** Panel (a) shows interior solutions, while panel (b) shows the maximum optimal level of avoidance a shipper will ever take when deviating from the cost-effective path is relatively inexpensive.

653 Now that the shipper's path decision is fully characterized, we turn to establishing the effect
 654 of the information set on optimal decisions. In particular, we want to establish how past en-
 655 counters affect the shippers decision making process today. In line with the empirical analysis,
 656 we will focus on the frequency of encounters for path x , which is given by the following ratio:

$$k(x) = \frac{|\mathbf{y} : y_i = x|}{|\mathbf{z} : z_j = x|}; \quad i \in \{1, \dots, n\}, j \in \{1, \dots, m\} \quad (\text{S9})$$

657 The expected effect of this observable on optimal paths is formalized in the proposition
 658 below:

659 **Proposition 2.** *The effect of the frequency of encounters, $k(x)$, on optimal path, x^* , is given by:*

$$\frac{\partial x^*}{\partial k(x)} = -\frac{\psi(pf)h\phi_{x\theta}(x^*, \theta)}{\psi(pf)h\phi_{xx}(x^*, \theta) + c''(x^*)} \frac{\partial \hat{\theta}}{\partial k(x)}, \quad \forall x \in \mathbb{X} \quad (\text{S10})$$

660 Proposition 2 is fairly intuitive: adjustments to optimal paths are linked to their effect in
 661 the estimated parameters of the probability function, as well as their effect on the probability
 662 of an encounter. In other words, marginal optimal adjustments incorporate any information
 663 regarding past encounters along the route to inform the expected probability of encounters. This
 664 information is then translated into the adjustments prescribed in Proposition 1. As a Corollary,
 665 the sign of this relationship is given by:

666 **Corollary 1.** *The direction of the effect of the frequency of encounters, $k(x)$, on optimal path,*
 667 *x^* , is given by the sign of the product:*

$$-\phi_{x\theta}(x^*, \hat{\theta}) \frac{\partial \hat{\theta}}{\partial k(x)} \quad (\text{S11})$$

668 The sign of the above relationship depends on two components: the cross derivative of the
 669 probability function, and the effect of observing more encounters along a given route on the
 670 estimate of θ . When this expression is positive, it is optimal to deviate more from the cost-
 671 effective path, while the opposite is true if the expression is negative. The reason why the sign
 672 switches relates to convexity of the probability of an encounter and the generality assumed for
 673 the relationship between the observed encounters and their effect on the probability estimate.

674 As an illustration, suppose encounters are observed farther from the cost-effective path.
 675 Operationally, this means an increase in the estimate for \bar{a} and a change in the slopes of the
 676 probability function for any x to the left of \bar{a} . The actual change will depend on the searching
 677 capability of the pirate. Consider the case in which the pirate can allocate only so much time
 678 to search every particular section of the feasible paths. The pirate searching farther implies a
 679 decrease in the intercept of $-\phi_x(x; \hat{\theta})\psi(pf)h$, or an increase in its slope, or both. Any of these
 680 changes effectively reflect a decrease in the probability of encountering the pirate. When this
 681 is the case, the intercept with the marginal cost shifts to the left, and thus less avoidance is
 682 optimal. Other responses will then be a function of how effective the pirate is when it comes to
 683 searching different sections of the path set.

684 Our main task is to establish the above relationship empirically in the main text. With this
 685 result, we are then able to estimate the cost of avoidance behavior in the shipping industry due
 686 to piracy. The characterization of the pirate's behavior is also provided for completeness.

687 S2.2.1 Optimal pirate behavior

In this section, we expand the theoretical insights of the main model to include the behavior
 of the pirate when deciding on how intensely to search for the target vessels. The working
 assumption of the model was that the pirate encounters occur whenever $b \geq pf$. The expected
 value of a successful encounter is then given by:

$$G(pf) = \int_{pf}^{\bar{b}} (b - pf) dF(b) \quad (\text{S12})$$

688 In this model, the pirate cannot directly observe the routing of the shipper, but he can still
 689 build an estimate. This estimate follows from observing past encounters, $\mathbf{y} = \{y_{(1)}, \dots, y_{(n)}\}$,
 690 and its own search effort, θ . Further, the pirate knows the probability of an encounter is given
 691 by $\phi(x, \theta)$. He is then able to estimate the path of the shipper and the associated probability of

692 an encounter as:

$$\hat{x} = \arg \max_x \{ \mathcal{L}(x; \theta, \mathbf{y}) \} \quad (\text{S13})$$

693 with $\mathcal{L}(x; \theta, \mathbf{y})$ as the likelihood function of $\phi(x; \theta)$. If the pirate has a search cost $s(\theta)$, which
694 is increasing in \bar{a} , the expected return to piracy is then given by:

$$R^p(\theta) = G(pf)\phi(\hat{x}, \theta) - s(\theta) \quad (\text{S14})$$

695 In addition, the pirate has a total time constraint, $h = b + t(\theta)$, with b denoting the time
696 working in non-pirate activities for wage w . $t(\theta)$ is a function that denotes the total time devoted
697 to searching for vessels. The pirate's concave utility of income is then given by:

$$u(m, \theta) = wb + R^p(\theta) \quad (\text{S15})$$

698 The time constraint can be rearranged as:

$$b = h - t(\theta) \quad (\text{S16})$$

699 and the utility function can be solely expressed as a function of θ as:

$$u(m, \theta) = w(h - t(\theta)) + R^p(\theta) \quad (\text{S17})$$

700 Taking partials with respect to θ and equalizing to zero gives:

$$-u'(\bullet)(bt'(\theta) + G(pf)\phi_{\theta}(\hat{x}, \theta)) = 0 \quad (\text{S18})$$

701 This expression defines optimal set adjustments for the pirate, which are captured by θ^* , and
702 implicitly defined by:

$$\phi_{\theta^*}(\hat{x}, \theta^*) = \frac{bt'(\theta^*)}{G(pf)} \quad (\text{S19})$$

703 This expression suggests that optimal pirate effort equates the marginal expected gain of
704 increasing the probability of an encounter with the marginal opportunity cost of working in
705 non-pirate activities. Following the same approach as with the shipper, it is straight forward to
706 show that the optimal pirate response to changes in the estimated path are given by:

$$\frac{\partial \theta^*}{\partial \hat{x}} = - \frac{\phi_{x\theta}(\hat{x}, \theta^*)}{\phi_{\theta\theta}(\hat{x}, \theta^*) - \frac{b}{G(pf)} t''(\theta)} \quad (\text{S20})$$

707 Our setting does not allow to sign the above expression. Nonetheless, with a few assumptions
708 regarding both the probability and the time requirement function, clear predictions associated
709 with the pirate behavior in the face of different observables are possible.

710 **S2.2.2 Proofs**

711 **Proposition 1**

712 *Proof.* The shipper's problem is given by:

$$\max_x \{ \pi - \phi(x, \hat{\theta}) \psi(pf) h - c(x) \} \quad (\text{S21})$$

713 Taking partials with respect to x and equalizing to zero:

$$-\phi_x(x, \hat{\theta}) \psi(pf) h - c'(x) = 0 \quad (\text{S22})$$

Rearranging and multiplying by minus one:

$$-\phi_x(x^*, \hat{\theta}) \psi(pf) h = c'(x^*) \quad (\text{S23})$$

714 Finally, $\hat{\theta}$ is estimated by examining the sequence of where past encounters took place, $\mathbf{y} =$
715 $\{y_1, \dots, y_n\}$, as:

$$\hat{\theta} = \arg \max_{\theta} \{ \mathcal{L}(\theta; \mathbf{y}, \mathbf{z}) \} \quad (\text{S24})$$

716 These two equations define the optimal path for the shipper based on past encounters, and
717 complete the proof. \square

718 **Lemma 1**

719 *Proof.* First, consider the case of zero avoidance, or $x^* = 0$. From the shipper's problem we
720 know that optimal deviation must satisfy:

$$\phi_x(x, \hat{\theta}) \psi(pf) h = -c'(x) \quad (\text{S25})$$

721 Because $c(x)$ is convex and $c(0) = 0$, it follows that $c'(0) = 0$. Substituting into the optimality
722 condition then gives:

$$\phi_x(0, \hat{\theta}) = 0 \quad (\text{S26})$$

723 which is equivalent to say that the only possibility for x to be equal to zero is if $\phi_x(0, \theta) = 0$,
724 which is never true by design.

725 Second, consider the case of total avoidance, or $x^* \geq \bar{a}$. Recall that

$$\phi_x(x, \theta) = 0 ; \forall x \geq \bar{a} \quad (\text{S27})$$

726 This condition implies that any deviation beyond \bar{a} renders no further reduction in the prob-
727 ability of an encounter. Because of the convexity of $c(x)$, it follows that any $x > \bar{a}$ is strictly
728 inferior to $x = \bar{a}$. Therefore, if $\nexists x \in [0, \bar{a}) : \phi_x(x, \hat{\theta}) \psi(pf) h = -c'(x)$, optimal decision
729 making dictates $x^* = \bar{a}$. All other scenarios are described by the optimality condition, which
730 completes the proof. \square

731 **Proposition 2**

Proof. Consider the optimality condition:

$$-\phi_x(x^*, \hat{\theta})\psi(pf)h = c'(x^*) \quad (\text{S28})$$

732 Totally differentiating with respect to $k(x)$ gives:

$$-\psi(pf)h \left(\phi_{xx}(x^*, \hat{\theta}) \frac{\partial x^*}{\partial k(x)} + \phi_{x\theta}(x^*, \hat{\theta}) \frac{\partial \hat{\theta}}{\partial k(x)} \right) = c''(x^*) \frac{\partial x^*}{\partial k(x)} \quad (\text{S29})$$

733 Rearranging with the respect to the partial effect on optimal routing x^* :

$$\frac{\partial x^*}{\partial k(x)} = - \frac{\psi(pf)h \phi_{x\theta}(x^*, \hat{\theta})}{\psi(pf)h \phi_{xx}(x^*, \hat{\theta}) + c''(x^*)} \frac{\partial \hat{\theta}}{\partial k(x)} \quad (\text{S30})$$

734 This equation characterizes the total effect of $k(x)$ on x^* , and completes the proof. \square

735 **Corollary 1**

736 *Proof.* The total effect of $k(x)$ on x^* is given by:

$$\frac{\partial x^*}{\partial k(x)} = - \frac{\psi(pf)h \phi_{x\theta}(x^*, \hat{\theta})}{\psi(pf)h \phi_{xx}(x^*, \hat{\theta}) + c''(x^*)} \frac{\partial \hat{\theta}}{\partial k(x)} \quad (\text{S31})$$

737 By design, $\phi_{xx}(x^*, \hat{\theta}) > 0$ and $c''(x^*) > 0$, which implies that the sign of the relationship be-
 738 tween $k(x)$ and x^* is completely characterized by the inverse of the product between $\phi_{x\theta}(x^*, \hat{\theta})$
 739 and $\partial \hat{\theta} / \partial k(x)$. This statement completes the proof. \square

740 **S2.3 Empirical challenges**

741 Establishing the effect of piracy on shipping behavior poses several challenges. One possi-
742 bility is a self-selection process that arises when pirates target specific ships, or it may be also
743 plausible that some vessels are actively looking to be hijacked. In the presence of any of these
744 possibilities, any estimate will be polluted with omitted variable bias.

745 For example, in Supplementary Text S2.1.2 we note that according to the documented testi-
746 monies, most of the initial encounters occur at random. In other words, pirates decide to attack
747 after observing the vessel that they happen to run into. The randomness behind these encounters
748 would normally be sufficient for identification, but the presence of sophisticated pirates chal-
749 lenges this claim. That is, it is plausible that the encounters could actually be planned by pirates
750 or the crew, which implies that they do not occur at random. This issue may be more likely to
751 occur in Southeast Asia, where the attacks appear to be more sophisticated.

752 The nature of the shipping industry, however, allows us to propose a solution for this prob-
753 lem. By most accounts, the shipping industry operates on a set schedule regardless of the type
754 of cargo or location. That is, the date at which vessels depart is pre-determined and plausibly
755 exogenous to pirate encounters in the past (39, 40). As these schedules are contracted years in
756 advance (40), the timing at which pirates encounters occur in the past is likely exogenous for
757 any given voyage departure. We construct the empirical model around this unique characteristic
758 of both the criminal activity, as well as the shipping industry. For robustness, however, we also
759 conduct an instrumental variable analysis in Supplementary Text S2.6.

760 Maritime transportation is also highly susceptible to weather conditions. It could be possible
761 that route adjustments after pirate encounters are merely a result of spurious correlation between
762 weather patterns and the timing of any given encounter. To account for this possibility, we
763 control for wind patterns along each individual voyage. Wind speed and direction are valid
764 controls for sailing weather conditions as, along with fetch (area of water over which the wind
765 blows), it determines the size of waves in the ocean (41).

766 **S2.4 Supporting material for regression analysis**

767 In this section, we provide supporting material for the regression analyses in the study. First,
768 we provide the tables with the summary statistics for the data used in the grid and voyage
769 analyses, respectively. Table S1 shows that the average traffic per grid is highly variable across
770 the globe, with the Gulf of Aden and Southeast Asia having much higher distance, occupancy
771 time, voyages and unique vessels transiting in their respective areas than the rest of the world
772 combined. For example, the average daily occupancy is 38.2 and 78.1 hours in the Gulf of Aden
773 and the Southeast Asia hotspots, respectively, while in the rest of the world the daily occupancy
774 is 35.1 hours instead. This pattern persists for all the variables in the dataset, though there is
775 considerable spread among all sub-samples and variables.

776 Table S2 shows that when analyzed at the voyage level, the pattern is slightly modified.
777 Here, in average, vessels crossing hotspots travel longer distances and for more time than vessels

table S1: Summary Statistics for Daily Ship Transit by Grid Cell.

	Distance (km)	Occupancy (hr)	Voyages (#)	Unique vessels (#)
Gulf of Aden				
Mean	708.6	38.2	14.3	14.1
SD	1,002.7	59.5	20.7	20.2
Median	126.4	9.4	3.0	3.0
Max	8,742.6	1,038.4	157.0	146.0
Gulf of Guinea				
Mean	137.8	11.9	3.3	3.3
SD	154.5	20.0	3.4	3.4
Median	97.8	5.8	3.0	2.0
Max	2,110.1	407.6	37.0	37.0
Southeast Asia				
Mean	1,085.3	78.1	18.5	17.6
SD	2,369.4	178.3	41.2	39.9
Median	247.0	20.8	4.0	4.0
Max	30,165.2	4,156.4	407.0	399.0
Rest of the World				
Mean	391.1	35.1	11.4	10.8
SD	919.6	79.1	26.6	25.4
Median	106.2	7.6	3.0	3.0
Max	16,593.6	2,172.6	261.0	247.0

table S2: Summary Statistics for Individual Voyage Features.

	Distance (km)	Time (hr)	Speed (km/hr)	Encounters (#/3 mo)
Gulf of Aden				
Mean	1,753.3	94.6	18.7	0.5
SD	3,060.6	217.5	7.4	1.2
Min	0.2	0.0	0.0	0.0
Max	421,538.8	37,861.1	115.5	25.0
Gulf of Guinea				
Mean	3,014.9	149.6	20.1	4.6
SD	4,040.2	238.4	7.5	5.8
Min	0.1	0.0	0.0	0.0
Max	468,276.4	33,372.3	58.6	45.0
Southeast Asia				
Mean	1,130.7	65.5	17.7	1.9
SD	2,768.4	266.8	6.6	5.0
Min	0.1	0.0	0.0	0.0
Max	813,656.8	51,409.2	130.2	44.0
Rest of the World				
Mean	608.8	30.9	21.5	0.1
SD	1,506.3	102.0	8.3	0.6
Min	0.0	0.0	0.0	0.0
Max	464,388.8	53,031.0	1,060.9	27.0

778 not crossing through hotspots, though there is also a relatively high degree of spread on the
779 voyage features. Importantly, the hotspots with the highest mean observed piracy encounters
780 in the preceding three months along routes take place in the Gulf of Guinea. The distribution
781 of the remaining variables in the analysis (i.e., costs and emissions) follow directly from these
782 observed features.

783 Second, we provide the regression tables not presented in the main text. The results for the
784 linear average effect of piracy are stacked in Table S4 for fuel, labor, and total operational costs
785 in thousands of US dollars, respectively. Across all samples, the results show that path adjust-
786 ments increase fuel cost the most. One additional encounter relates to hundreds or thousands
787 of dollars in additional fuel spent. These estimates are consistent with path adjustments. The
788 results also suggest that vessels passing through the Gulf of Aden face the biggest burden with
789 an additional US\$5 thousand per encounter, while those in the Southeast Asia face the least.

790 These adjustments are also meaningful in terms of labor cost. The effects of additional
791 encounters are positive and significant, but at most half of the adjustment cost when compared
792 to additional fuel consumption. We note that this result is consistent across samples.

table S3: Effect of Past Pirate Encounters on Shipping Cost.

	Global	G. of Aden	G. of Guinea	S.E. Asia
<i>Panel (A): Fuel Cost (TUSD)</i>				
Encounters (3 mo)	0.58*** (0.08)	5.12*** (0.58)	0.41*** (0.06)	0.49*** (0.12)
<i>Panel (B): Labor Cost (TUSD)</i>				
Encounters (3 mo)	0.26*** (0.03)	1.31*** (0.12)	0.25*** (0.02)	0.23*** (0.04)
<i>Panel (C): Total Cost (TUSD)</i>				
Encounters (3 mo)	0.83*** (0.11)	6.43*** (0.66)	0.66*** (0.07)	0.72*** (0.14)
Observations	25,628,927	1,034,194	276,183	6,334,875
Hotspot FE	X	●	●	●

* p < 0.1, ** p < 0.05, *** p < 0.01 The unit of observation is a voyage. Each panel examines a calculated cost in terms of fuel cost, labor cost, and total cost as the sum of both. All coefficients are in thousands of US\$. The sample spans from 2013 to 2021. Every column is a different sample: Global is the analysis using the whole sample. G. of Aden, S.E. Asia, and G. of Guinea restrict the sample to vessels passing through one of the hotspots, respectively. Every panel-column combination is a different regression analysis. Encounters (3mo) is the count of pirate encounters recorded in the projected path of the vessel in the preceding 90 days from the departure date using a 5 degree spatial footprint. Controls include average wind speed along the voyage and the wind-resistance index. Fixed effects include country-to-country combination, vessel type, vessel size, hotspot, and a battery of month by year and top port-to-port combination for country-to-country combination dummies.

table S4: Effect of Past Pirate Encounters on Shipping Cost.

	Global	G. of Aden	G. of Guinea	S.E. Asia
<i>Panel (A): Fuel Cost (TUSD)</i>				
Encounters (3 mo)	0.58*** (0.08)	5.12*** (0.58)	0.41*** (0.06)	0.49*** (0.12)
<i>Panel (B): Labor Cost (TUSD)</i>				
Encounters (3 mo)	0.26*** (0.03)	1.31*** (0.12)	0.25*** (0.02)	0.23*** (0.04)
<i>Panel (C): Total Cost (TUSD)</i>				
Encounters (3 mo)	0.83*** (0.11)	6.43*** (0.66)	0.66*** (0.07)	0.72*** (0.14)
Observations	25,628,927	1,034,194	276,183	6,334,875
Hotspot FE	X	•	•	•

* $p < 0.1$, ** $p < 0.05$, *** $p < 0.01$ The unit of observation is a voyage. Each panel examines a calculated cost in terms of fuel cost, labor cost, and total cost as the sum of both. All coefficients are in thousands of US\$. The sample spans from 2013 to 2021. Every column is a different sample: Global is the analysis using the whole sample. G. of Aden, S.E. Asia, and G. of Guinea restrict the sample to vessels passing through one of the hotspots, respectively. Every panel-column combination is a different regression analysis. Encounters (3mo) is the count of pirate encounters recorded in the projected path of the vessel in the preceding 90 days from the departure date using a 5 degree spatial footprint. Controls include average wind speed along the voyage and the wind-resistance index. Fixed effects include country-to-country combination, vessel type, vessel size, hotspot, and a battery of month by year and top port-to-port combination for country-to-country combination dummies.

793 We estimate the effect of piracy on total operational costs by aggregating both fuel and
794 labor costs. These results are reported in Panel (C) of Table S4, and suggest that the average
795 increase in operational costs due to avoidance measures per additional encounter ranges from
796 over US\$600 in the Gulf of Guinea to over US\$6.4 thousand in the Gulf of Aden. Globally, this
797 effect averages down to about US\$800 for each additional pirate encounter.

798 The linear average effects of piracy on emissions are stacked in Table S5 for CO₂, NO_x,
799 and SO_x, respectively. As expected from previous results, excessive fuel consumption leads to
800 excessive emissions across the spectrum of relevant pollutants. In particular, increases in CO₂
801 range from 2.6 to 35.15 tons per voyage per past pirate encounter. NO_x and SO_x emissions due
802 to piracy are relatively less voluminous, though this is a direct consequence of their significantly
803 smaller concentrations in bunker fuel relative to carbon. Nonetheless, regression estimates point
804 to dozens of kilograms, and hundreds in the case of the Gulf of Aden, of excess pollutants
805 emitted due to the presence of pirates.

table S5: Effect of Past Pirate Encounters on Shipping Emissions.

	Global	G. of Aden	G. of Guinea	S.E. Asia
<i>Panel (A): CO₂ (tons)</i>				
Encounters (3 mo)	3.50*** (0.37)	35.15*** (3.85)	4.29*** (0.39)	2.60*** (0.36)
<i>Panel (B): NO_x (kg)</i>				
Encounters (3 mo)	85.70*** (9.29)	895.31*** (99.26)	106.15*** (10.00)	62.67*** (8.96)
<i>Panel (C): SO_x (kg)</i>				
Encounters (3 mo)	72.95*** (7.79)	731.85*** (80.07)	89.29*** (8.17)	54.23*** (7.55)
Observations	25,629,585	1,034,211	276,220	6,335,025
Hotspot FE	X	•	•	•

* p < 0.1, ** p < 0.05, *** p < 0.01 The unit of observation is a voyage. Each panel examines a calculated emission in terms of *textCO₂* (tons), NO_x (kg), and SO_x (kg). The sample spans from 2013 to 2021. Every column is a different sample: Global is the analysis using the whole sample. G. of Aden, S.E. Asia, and G. of Guinea restrict the sample to vessels passing through one of the hotspots, respectively. Every panel-column combination is a different regression analysis. Encounters (3mo) is the count of pirate encounters recorded in the projected path of the vessel in the preceding 90 days from the departure date using a 5 degree spatial footprint. Controls include average wind speed along the voyage and the wind-resistance index. Fixed effects include country-to-country combination, vessel type, vessel size, hotspot, and a battery of month by year and top port-to-port combination for country-to-country combination dummies.

806 **S2.5 Counterfactual costs and emissions**

807 We use the fully specified *global* model (5° grid, 3 month window) to predict voyage-level
808 fuel and labor costs, as well as emissions of CO_2 , NO_x , and SO_x . We make predictions using
809 the observed number of pirate encounters and a counterfactual of no pirate encounters at all.
810 We then take the difference between these two predictions to obtain a voyage-level estimate
811 of the additional fuel and labor costs, and emissions of each pollutant. We then calculate the
812 total annual costs and emissions across all voyages. These results are shown in Table S6 and
813 Table S7, where we also provide information disaggregated by hotspot.

814 Having matched each voyage to its additional costs and emissions, we then divide a voyage's
815 cost (or emissions) across all $0.5^\circ \times 0.5^\circ$ grid cells along which the vessel transited. For each grid
816 cell, we calculate the total surplus costs (fuel + labor) or emissions of each pollutant. We then
817 take the average across all years (2013-2021) and use these data to produce maps shown in
818 Figure 3A.

819 We are also interested in estimating the total public and private costs of modern-day piracy.
820 We monetize the environmental impacts caused by additional emission of local and global air
821 pollutants using their social-cost. Specifically, we use estimates provided by the Interagency
822 Working Group on Social Cost of Greenhouse Gases (11), which suggest that an additional ton
823 of CO_2 or NO_x induce damages valued at US\$51 and US\$18,000 (in 2020 US\$ assuming a
824 3% discount rate). For SO_x we use estimates from Mier, Adelowo, and Weissbart (12), which
825 indicates an additional ton of SO_2 inducing damages of US\$14,694 (in 2020 US\$). We then
826 aggregate all information by ASAM region, and produce bar charts shown in Figure 3B.

table S6: Total Costs of Piracy to the Shipping Industry.

	2013	2014	2015	2016	2017	2018	2019	2020	2021
Fuel (Million USD)									
Global	1,099	1,274	1,571	988	1,036	553	478	1,325	1,210
G. of Aden	50	34	18	42	66	17	23	42	38
G. of Guinea	108	75	52	91	82	106	51	114	72
Southeast Asia	838	1,129	1,431	619	663	319	327	1,032	914
Labor (Million USD)									
Global	491	569	702	442	463	247	214	592	541
G. of Aden	22	15	8	19	29	7	10	19	17
G. of Guinea	48	34	23	41	37	47	23	51	32
Southeast Asia	374	505	640	277	297	142	146	461	409
Total (Million USD)									
Global	1,590	1,843	2,273	1,430	1,499	801	692	1,917	1,751
G. of Aden	72	49	26	61	95	24	33	61	55
G. of Guinea	156	109	75	131	119	153	74	164	104
Southeast Asia	1,212	1,634	2,072	896	960	461	473	1,493	1,323

table S7: Total Emission of Air Pollutants due to Piracy

	2013	2014	2015	2016	2017	2018	2019	2020	2021
CO₂ (Thousand metric tons)									
Global	5,325	6,226	7,622	4,740	5,144	2,727	2,356	6,479	5,968
G. of Aden	239	159	91	204	310	80	114	201	182
G. of Guinea	528	369	257	449	408	511	248	547	344
Southeast Asia	4,040	5,508	6,919	2,994	3,262	1,548	1,597	5,055	4,456
NO_x (Metric tons)									
Global	130,242	152,280	186,422	115,938	125,818	66,712	57,625	158,464	145,986
G. of Aden	5,840	3,883	2,223	4,985	7,581	1,962	2,796	4,926	4,446
G. of Guinea	12,919	9,036	6,295	10,974	9,983	12,502	6,062	13,379	8,412
Southeast Asia	98,808	134,736	169,240	73,237	79,781	37,861	39,073	123,644	108,991
SO_x (Metric tons)									
Global	110,861	129,620	158,682	98,686	107,096	56,786	49,051	134,885	124,263
G. of Aden	4,971	3,305	1,892	4,243	6,453	1,670	2,380	4,193	3,784
G. of Guinea	10,996	7,691	5,359	9,341	8,497	10,642	5,160	11,388	7,161
Southeast Asia	84,105	114,687	144,057	62,339	67,909	32,227	33,258	105,245	92,773

827 **S2.6 Instrumental variable analysis**

828 In the main analysis, our identification assumption relies on the timing of shipping vessel depar-
829 tures. We assume that these are exogenous to the number of encounters in the preceding months
830 due to shipment schedules. Nonetheless, as described in Supplementary Text S2.3, there is still
831 a chance that sophisticated pirates or shippers might be self-selecting into treatment, thereby
832 violating our exogeneity assumption.

833 To alleviate these concerns, we conduct an ancillary analysis that relies on an instrumental
834 variable approach. Here, we will focus on the two hotspots that afflict the African continent, as
835 they are relatively more condensed geographically and follow a similar business model. We con-
836 jecture that political stability is correlated with reported pirate encounters within the Economic
837 Exclusive Zones (EEZ) comprising the Gulf of Aden and the Gulf of Guinea, respectively. This
838 is consistent with previous studies on economic stability and the incidence of piracy (33, 34). In
839 turn, political stability is only likely to affect a vessel’s path through piracy.

840 First, we characterize the Gulf of Aden as the EEZs of Djibouti, Eritrea, Eritrea, Kenya,
841 Kenya, Oman, Somalia, Tanzania, and Yemen. The Gulf of Aden is characterized by the EEZs
842 of Angola, Benin, Cameroon, Equatorial Guinea, Gabon, Ghana, Liberia, Nigeria, Sao Tome
843 and Principe, Sao Tome and Principe, and Togo. We then count the total number of pirate
844 encounters, and use the observed vessel monitoring data from Global Fishing Watch for our
845 sample of shipping vessels to summarize the total transit time (hr), distance traveled (km), and
846 number of unique vessels that were observed annually in each EEZ from 2013 to 2021.

847 We then take data from the World Bank’s Worldwide Development Indicators and track the
848 Political Stability Index by country, which assesses the likelihood of government destabilization
849 or overthrow through unconstitutional or violent means, including terrorism.¹² The index ag-
850 gregates perceptions from various sources, including surveys and expert evaluations, and ranges
851 from -2.5 (indicating low stability) to 2.5 (high stability). Summary statistics for the variables
852 used in the analysis is shown in Table S8.

The analysis is implemented in two stages. The first stage is as follows:

$$TNE_{it} = \Lambda + \Phi PS_{it} + \Psi_i + \Pi' X_t + u_{it} \quad (\text{S32})$$

853 TNE is the number of encounters, while PS is the reported political stability in country i in
854 year t , respectively. Φ is the marginal change in yearly pirate encounters that follows a change
855 in political stability. Ψ is an indicator variable that takes a value of one if the country belongs
856 to the Gulf of Guinea. X_t is a dummy variable for year t . To account for potential geographical
857 and temporal correlation, we cluster standard errors by hotspot by year.

858 In the second stage we are interested in the number of vessels that go through EEZ, the
859 distance they travel within EEZs (km/vessel), and the time they spend in said EEZ (hr/vessel),
860 as a function of the pirate encounters in that area. The model is as follows:

¹²In addition to political stability, the World Bank tracks a variety of indicators that relate to the economic and institutional stability of countries worldwide. These data updated on a yearly basis and are estimated by country. The data are available online here: <https://t.ly/UbR6y>

table S8: Summary Statistics for Variables Used in the Instrumental Variable Analysis.

	Political Stability	Encounters (#)	Vessels (#)	Distance (km/vessel)	Time (hr/vessel)
Gulf of Aden					
Mean	-1.0	2.6	3,857.6	1,446.6	76.0
SD	1.0	5.1	3,148.3	1,277.3	59.2
Min	-3.0	0.0	212.0	30.5	1.2
Max	0.8	36.0	9,958.0	4,547.0	190.1
Gulf of Guinea					
Mean	-0.4	5.8	1,896.7	1,045.5	65.3
SD	0.7	11.6	721.6	607.6	36.8
Min	-2.1	0.0	660.0	247.0	11.3
Max	0.6	67.0	3,736.0	2,248.5	144.7

table S9: First Stage IV Regression: Effect of Political Stability on Yearly Pirate Encounters.

	(1)	(2)	(3)	(4)
Political Stability	-3.72*** (1.17)	-3.73*** (1.20)		-5.07*** (1.40)
Gulf of Guinea Dummy			3.12*** (0.54)	6.47*** (0.93)
Year FE		X	X	X

* p < 0.1, ** p < 0.05, *** p < 0.01 The unit of observation is a country. The sample spans from 2013 to 2021. Every column is a different specification. Political Stability is the index reported by the World Bank as part of its World Development Indicators. Additional covariates include a dummy variable if a country belongs to the Gulf of Guinea and yearly dummies. Standard errors are clustered by gulf by year. Number of observations is 180.

$$y_{it} = \alpha + \beta \widehat{TNE}_{it} + \Psi_i + \Pi' X_t + e_{it} \quad (S33)$$

861 y is the shipping measure of interest, while \widehat{TNE}_{it} is the predicted number of encounters
862 in the first stage in country i in year t . To account for potential geographical and temporal
863 correlation, we continue to cluster standard errors by hotspot by year.

864 The results of the analysis are presented in Tables S9 and S10, respectively. Table S10 also
865 shows the result for a simple ordinary least squares (OLS) for reference. Overall, the analysis
866 provides support for the validity of the instrument in the first stage. Increases in political stabil-
867 ity are correlated with a decrease in pirate encounters in a given EEZ (Table S9). This result is
868 robust to the inclusion of the Gulf of Guinea dummy, and it highlights the potential importance
869 of a country's economic and institutional state when it comes to the proliferation of piracy.

table S10: Instrumental Variable Analysis of the Effect of Pirate Encounters on Shipping Patterns

	OLS			2SLS		
	(1)	(2)	(3)	(4)	(5)	(6)
<i>Panel (A): Vessels (#)</i>						
Encounters	9.93 (12.73)	9.41 (10.56)	28.25* (13.49)	-22.01 (37.47)	-24.17 (36.53)	-113.53** (48.67)
<i>Panel (B): Distance (km/vessel)</i>						
Encounters	19.03** (7.18)	19.60** (7.01)	23.98** (8.33)	83.26** (30.33)	83.33** (31.12)	52.01** (18.79)
<i>Panel (C): Time (hr/vessel)</i>						
Encounters	1.45*** (0.23)	1.51*** (0.23)	1.65*** (0.28)	4.59*** (1.26)	4.60*** (1.28)	3.41*** (0.80)
Gulf of Guinea Dummy			X			X
Year FE		X	X		X	X
F-Stat				25.73	25.56	46.20

* p < 0.1, ** p < 0.05, *** p < 0.01 The unit of observation is a country. Each panel examines an observed feature in terms of total number of vessels transiting an EEZ (#), total normalized distance traveled within an EEZ (hr/vessel), and total normalized time spent within an EEZ (hr/vessel). The explanatory variable is number of pirate encounters. The sample spans from 2013 to 2021. Columns (1) to (3) present the results of ordinary least squares (OLS), while columns (4) to (5) present the result from a two-stage least squares using political stability as an instrument for pirate encounters, respectively. Every panel-column combination is a different regression analysis. Additional covariates include a dummy variable if a country belongs to the Gulf of Guinea and yearly dummies. Standard errors are clustered by gulf by year. Number of observations is 180.

870 The instrumental variable analysis in Table S10 provides several insights. First, the re-
871 sults are consistent with the main analysis. That is, travel distance and time, per vessel, are
872 increased in the presence of piracy, at least at the EEZ level. These increases follow our the-
873 oretical insights in Supplementary Text S2.2. We note, however, that there also seems to be a
874 significant decrease in shipping EEZ total traffic following pirate encounters after accounting
875 for geographical patterns across hotspots.

876 Compared with the OLS analysis, these estimates also suggest that failing to account for
877 endogeneity can create a few issues. First, simple OLS would suggest that there are more
878 vessels sailing in these EEZs. The instrumental variable estimates show that the relationship
879 is negative instead. Second, and while the estimates have the right sign, that OLS tends to
880 underestimate the level of adjustment within EEZs.

881 These results do not replace the insights in the main paper but tell a cohesive story. Captains
882 are aware of the risk that pirates represent and adjust their paths accordingly. Increases in
883 operational cost and emissions follow directly from these results.

884 **S2.7 Robustness tests**

885 Here, we show robustness checks for all of the empirical results: how pirate encounters affect
886 total shipping traffic within spatial grids, and how pirate encounters affect the features of in-
887 dividual voyages. The two sets of robustness checks largely follow the same pattern. Pirate
888 encounters reduce traffic within grid cells. These adjustments result in adjustments at the indi-
889 vidual voyage level, which is then demonstrated by increase in the average total distance time
890 traveled for the same port-to-port combination.

891 **S2.7.1 Grid-level analysis**

892 Here, we show evidence of the robustness of the grid-level analysis. First, we show robustness
893 to different sets of fixed effects in tabular form. The first set of results uses a global sample (Ta-
894 ble S11). Then, we repeat the exercise for the subset of grid cells belonging to each of the three
895 hotspots. The results for the Gulf of Aden, Gulf of Guinea, and Southeast Asia are presented
896 in Table S12, Table S13, and Table S14, respectively. In all tables, the fourth column presents
897 the same results as Table 1 in the main text, which are the preferred specification including
898 fixed-effects for grid id, for ASAM subregion, and for ASAM region by year by month. All
899 estimates from models with at least one fixed effect are relatively stable, with estimates always
900 showing the same direction and similar magnitude as the preferred specification.

901 Second, we show robustness to using the total number of encounters occurring in a grid
902 cell over the last 3, 6 and 12 months. We find consistent evidence that additional past pirate
903 encounters result in reduced vessel activity globally and across all three hotspots (Figure S2).
904 Additionally, lengthening the time window for encounters reduces the coefficient estimates be-
905 cause encounters far into the past are not as important as recent events.

906 Finally, as stated in our Methods, we also estimate dynamic effects in an event-study frame-
907 work. Here, we use distance traveled (km), normalized distance traveled (km/vessel and km/voyage),
908 occupancy time (hr), and normalized occupancy time (hr/vessel and hr/voyage) as our response
909 variables. This analysis restricts the sample to grid cells with no overlapping attacks five days
910 before or after a given attack date ($N = 233$). The main results are shown in Figure S3. As
911 before we also test for different fixed-effect specifications (Figure S4) and effects by hotspot
912 (Figure S5). The results are generally consistent and show a decrease in grid-level activity
913 following, but not leading to, an encounter.

table S11: Effect of Piracy on Grid-level Ship Transit For Different Fixed-effects Specifications for a Global Sample.

	(1)	(2)	(3)	(4)
<i>Panel (A): Total Distance (km)</i>				
Encounters (3 mo)	484.96* (284.26)	-14.76 (12.53)	-14.76 (12.53)	-4.90 (11.53)
<i>Panel (B): Occupancy (hr)</i>				
Encounters (3 mo)	58.73* (31.50)	7.75 (6.86)	7.75 (6.86)	8.42 (6.73)
<i>Panel (C): Voyages (#)</i>				
Encounters (3 mo)	10.05* (5.94)	-0.06 (0.47)	-0.06 (0.47)	0.32 (0.44)
<i>Panel (D): Vessels (#)</i>				
Encounters (3 mo)	9.83* (5.85)	-0.03 (0.48)	-0.03 (0.48)	0.35 (0.45)
Grid ID FE		X	X	X
ASAM Subregion FE			X	X
ASAM Region-year-month FE				X

* $p < 0.1$, ** $p < 0.05$, *** $p < 0.01$ The unit of observation is a grid cell ($N = 590$ unique cells). The sample spans from 2013 to 2021. Each panel examines a measure of grid-level ship transit in terms of total distance in kilometers (km), total occupancy time in hours (hr), and the number of unique voyages or vessels transiting through the grid cell. Each column is a different regression analysis adding fixed-effects by grid ID, then group, and finally time. Every panel-column combination is a different regression analysis. Encounters (3mo) is the count of pirate encounters recorded within the grid cell in the preceding 90 days. Numbers in parentheses are Conley Standard Errors (100 km cutoff). Number of observations: 1,939,330.

table S12: Effect of Piracy on Grid-level Ship Transit For Different Fixed-effects Specifications for the Gulf of Aden.

	(1)	(2)	(3)	(4)
<i>Panel (A): Total Distance (km)</i>				
Encounters (3 mo)	58.07 (105.55)	-30.57** (14.67)	-30.57** (14.67)	-26.50* (13.78)
<i>Panel (B): Occupancy (hr)</i>				
Encounters (3 mo)	7.91** (3.84)	-0.89 (1.05)	-0.89 (1.05)	-0.70 (1.20)
<i>Panel (C): Voyages (#)</i>				
Encounters (3 mo)	0.61 (1.24)	-1.05** (0.45)	-1.05** (0.45)	-0.67** (0.34)
<i>Panel (D): Vessels (#)</i>				
Encounters (3 mo)	0.62 (1.24)	-1.04** (0.44)	-1.04** (0.44)	-0.65* (0.34)
Grid ID FE		X	X	X
ASAM Subregion FE			X	X
ASAM Region-year-month FE				X

* p < 0.1, ** p < 0.05, *** p < 0.01 The unit of observation is a grid cell (N = 93 unique cells). The sample spans from 2013 to 2021. Each panel examines a measure of grid-level ship transit in terms of total distance in kilometers (km), total occupancy time in hours (hr), and the number of unique voyages or vessels transiting through the grid cell. Each column is a different regression analysis adding fixed-effects by grid ID, then group, and finally time. Encounters (3mo) is the count of pirate encounters recorded within the grid cell in the preceding 90 days. Numbers in parentheses are Conley Standard Errors (100 km cutoff). Number of observations: 305,691.

table S13: Effect of Piracy on Grid-level Ship Transit For Different Fixed-effects Specifications for the Gulf of Guinea.

	(1)	(2)	(3)	(4)
<i>Panel (A): Total Distance (km)</i>				
Encounters (3 mo)	28.59 (23.12)	-4.80*** (1.64)	-4.80*** (1.64)	-4.58*** (1.32)
<i>Panel (B): Occupancy (hr)</i>				
Encounters (3 mo)	6.84 (4.69)	-0.33 (0.63)	-0.33 (0.63)	-0.26 (0.62)
<i>Panel (C): Voyages (#)</i>				
Encounters (3 mo)	0.94 (0.64)	-0.10*** (0.03)	-0.10*** (0.03)	-0.11*** (0.04)
<i>Panel (D): Vessels (#)</i>				
Encounters (3 mo)	0.91 (0.63)	-0.10*** (0.03)	-0.10*** (0.03)	-0.10*** (0.04)
Grid ID FE		X	X	X
ASAM Subregion FE			X	X
ASAM Region-year-month FE				X

* p < 0.1, ** p < 0.05, *** p < 0.01 The unit of observation is a grid cell (N = 134 unique cells). The sample spans from 2013 to 2021. Each panel examines a measure of grid-level ship transit in terms of total distance in kilometers (km), total occupancy time in hours (hr), and the number of unique voyages or vessels transiting through the grid cell. Each column is a different regression analysis adding fixed-effects by grid ID, then group, and finally time. Encounters (3mo) is the count of pirate encounters recorded within the grid cell in the preceding 90 days. Numbers in parentheses are Conley Standard Errors (100 km cutoff). Number of observations: 440,458.

table S14: Effect of Piracy on Grid-level Ship Transit For Different Fixed-effects Specifications for Southeast Asia.

	(1)	(2)	(3)	(4)
<i>Panel (A): Total Distance (km)</i>				
Encounters (3 mo)	773.99*** (266.27)	-21.09 (21.06)	-21.09 (21.06)	-3.69 (21.18)
<i>Panel (B): Occupancy (hr)</i>				
Encounters (3 mo)	91.82*** (34.42)	14.70 (10.35)	14.70 (10.35)	15.97 (9.89)
<i>Panel (C): Voyages (#)</i>				
Encounters (3 mo)	16.56*** (5.87)	0.14 (0.79)	0.14 (0.79)	0.79 (0.68)
<i>Panel (D): Vessels (#)</i>				
Encounters (3 mo)	16.22*** (5.79)	0.21 (0.80)	0.21 (0.80)	0.83 (0.69)
Grid ID FE		X	X	X
ASAM Subregion FE			X	X
ASAM Region-year-month FE				X

* p < 0.1, ** p < 0.05, *** p < 0.01 The unit of observation is a grid cell (N = 149 unique cells). The sample spans from 2013 to 2021. Each panel examines a measure of grid-level ship transit in terms of total distance in kilometers (km), total occupancy time in hours (hr), and the number of unique voyages or vessels transiting through the grid cell. Each column is a different regression analysis adding fixed-effects by grid ID, then group, and finally time. Encounters (3mo) is the count of pirate encounters recorded within the grid cell in the preceding 90 days. Numbers in parentheses are Conley Standard Errors (100 km cutoff). Number of observations: 489,763.

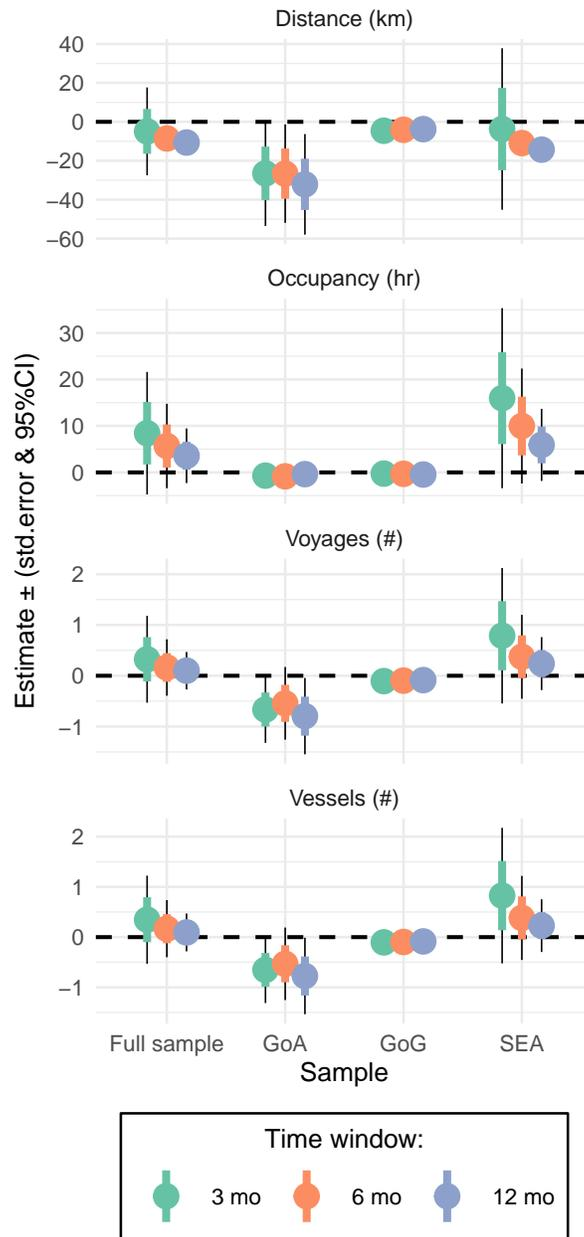


fig S2: **Average piracy effect on grid-level ship transit.** The x-axis shows the sub-sample and the y-axis the estimated effect. Each marker indicates a coefficient estimate for the average effect of the number of attacks over the last 3, 6, or 12 months on the measure of ship transit shown in each panel. The colored portion of error bars show standard errors and the black portion of the error bars shows 95% CIs. Note how increasing the time window results in attenuated coefficients.

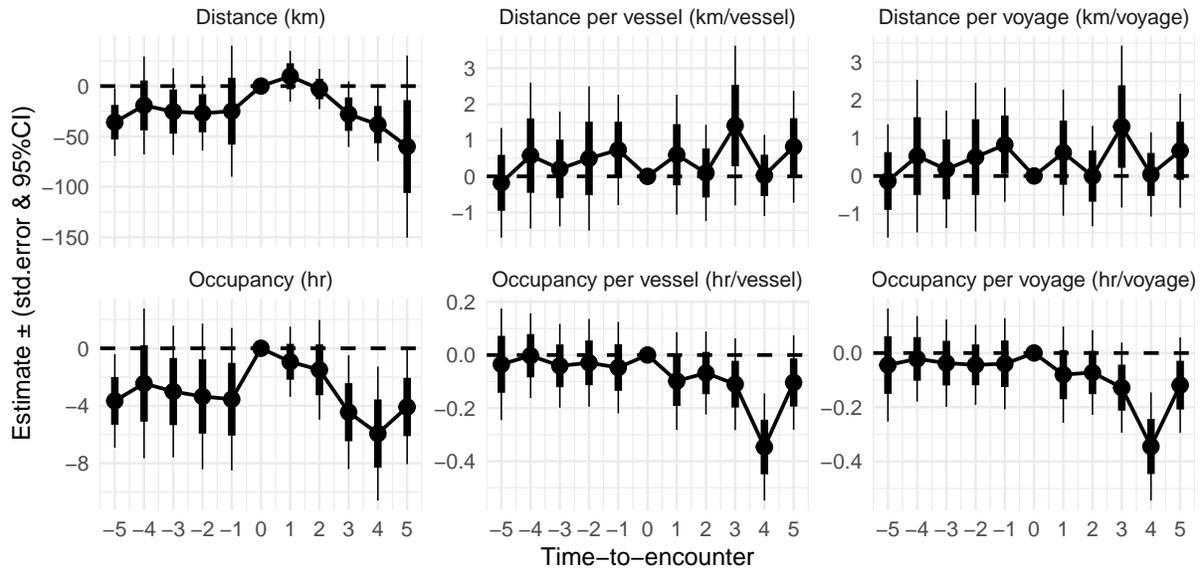


fig S3: **Event-study for the effect of piracy attacks on ship transit.** The top row shows coefficient estimates with distance (km) and normalized distance (km/vessel and km/voyage) as the dependent variable. The bottom row uses occupancy time (hours) and normalized occupancy time (hr/vessel and hr/voyage) as the dependent variable. We estimate a total of 10 coefficients and our sample contains 233 grid cells. Coefficients show the change in transit relative to the day of attack (i.e., Time-to-encounter = 0). The thick portion of error bars are spatial Conley standard errors using a 100 km radius and the thin portion of error bars shows 95% CIs. All estimations include fixed effects by ASAM subregion, Year-by-month-by-ASAM region, and grid-id.

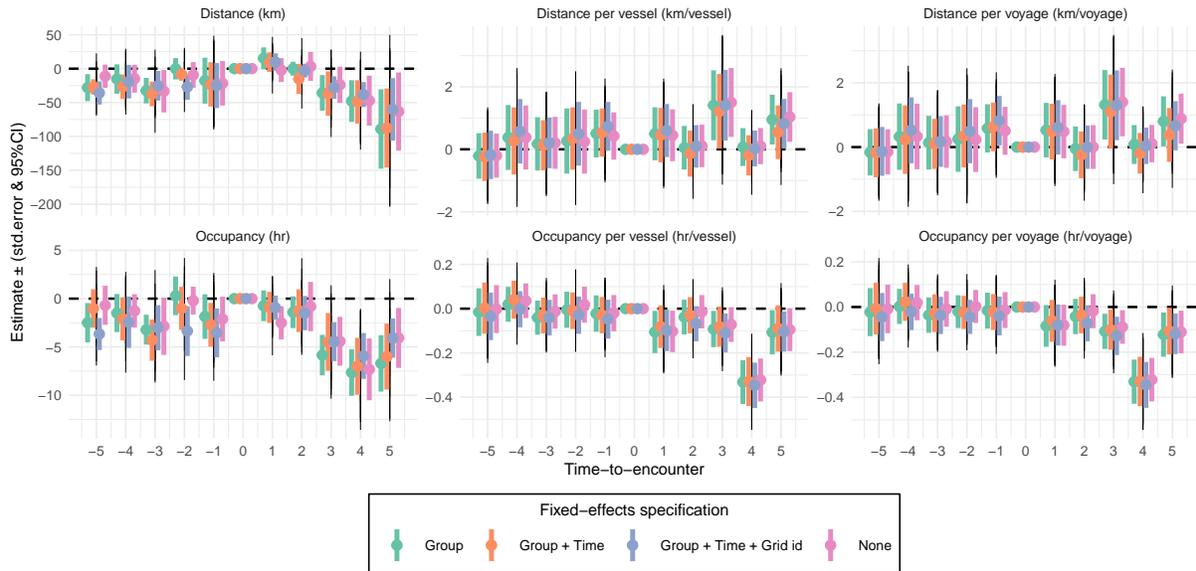


fig S4: **Build-up to a Two-way fixed effects specification.** The top row shows coefficient estimates with distance (km) and normalized distance (km/vessel and km/voyage) as the dependent variable. The bottom row uses occupancy time (hours) and normalized occupancy time (hr/vessel and hr/voyage) as the dependent variable. We estimate a total of 10 coefficients and our sample contains 233 grid cells. Coefficients show the change in transit relative to the day of attack (i.e., Time-to-encounter = 0). Colors indicate different fixed-effects specification. The thick portion of error bars are spatial Conley standard errors using a 100 km radius and the thin portion of error bars shows 95% CIs. The preferred specification contains fixed-effects for group, time, and observational unit and are equivalent to these shown in Figure S3.

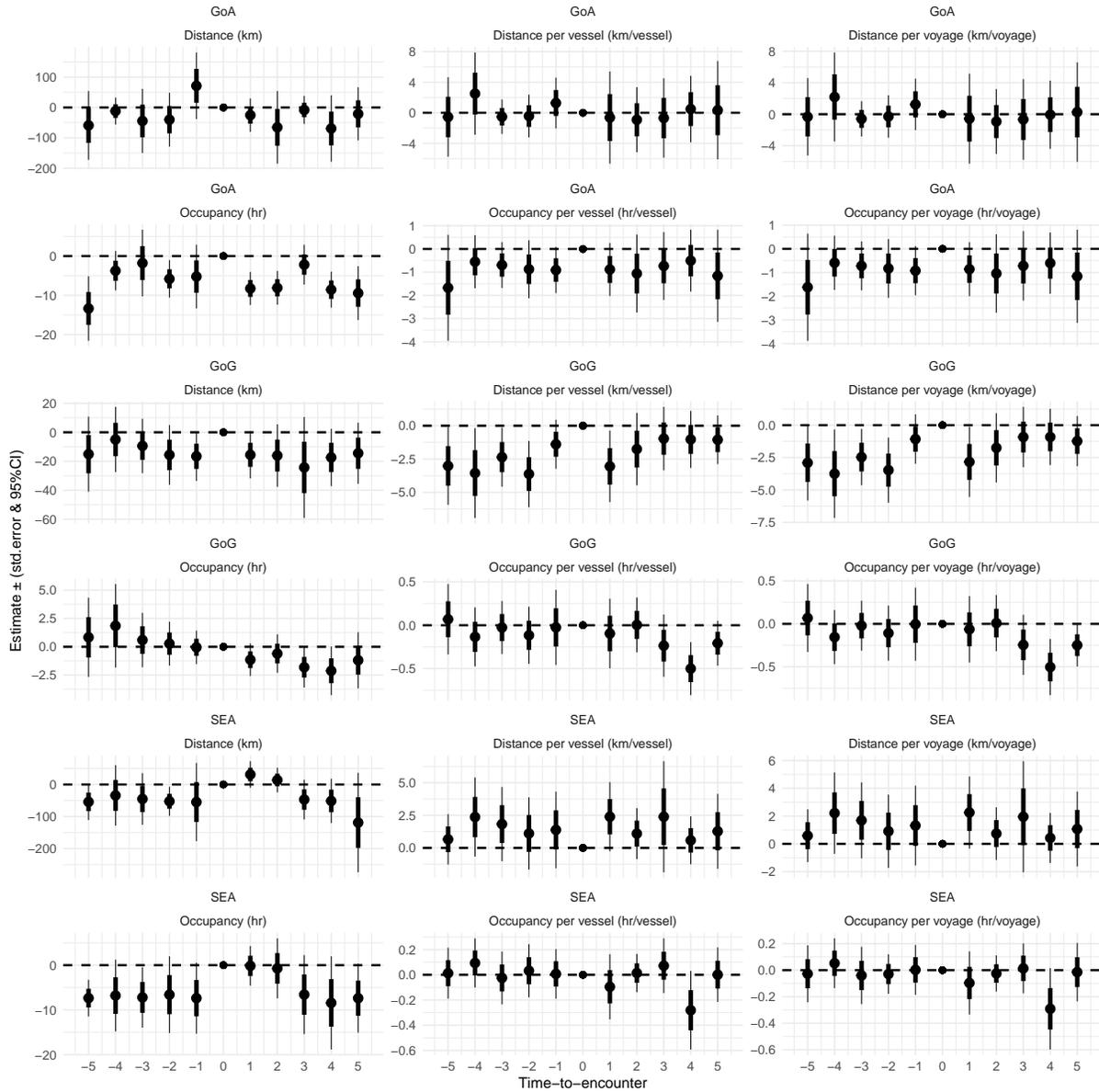


fig S5: Event-study for the effect of piracy attacks on ship transit by hotspot. Each row shows a combination of hotspot - measure. We estimate a total of 10 coefficients, which show the change in transit relative to the day of attack (i.e., Time-to-encounter = 0). The thick portion of error bars are spatial Conley standard errors using a 100 km radius and the thin portion of error bars shows 95% CIs. All estimations include fixed effects by ASAM subregion, Year-by-month-by-ASAM region, and grid-id.

914 **S2.7.2 Voyage-level analysis**

915 Here we present evidence of the robustness of the voyage analysis to several modeling assump-
916 tions. First, we show robustness to different sets of fixed effects in tabular form. The estimates
917 are sensitive to the inclusion of country-to-country fixed effects, but this is expected as the
918 length and specific paths of each route are bound to vary widely across combinations. The suite
919 of results are included in Tables S15 to S23. Overall, the results are highly robust to the addi-
920 tion of vessel, hotspot and top route fixed effects. The results are also robust to the inclusion of
921 weather controls in the form of wind speed and wind-resistance index.

922 Second, we show robustness to i) using a rolling window of 3, 6, and 12 months, as well as
923 the use of a global $3^{\circ} \times 3^{\circ}$, $5^{\circ} \times 5^{\circ}$, and $7^{\circ} \times 7^{\circ}$ grid to construct the past encounters variable. This
924 approach allows us to test the temporal and spatial sensitivity of our analysis and the results
925 are shown in Figure S6. The results show that the effect of recent encounters diminishes when
926 longer time windows are considered and that working with larger spatial footprints (i.e., $7^{\circ} \times 7^{\circ}$)
927 tends to attenuate results toward zero. For completeness, we will maintain these sensitivities in
928 all of the analyses below.

929 Third, we show robustness of the results to the categorization of cargo vessels. In the main
930 analysis, we use the best available vessel class for each individual vessel as categorized by
931 Global Fishing Watch. This ‘best available’ approach uses the vessel class provided by official
932 registries where available, and infers vessel class using a neural network when registries are not
933 available (9). As a robustness check, we restrict the analysis to work with: 1) vessels that are
934 always categorized as cargo vessels according to official registries; as well as 2) expand it as
935 those who are categorized in official registries as being cargo vessels at least once. These results
936 are shown in Figure S7 and Figure S8 and are virtually unchanged with respect to the results in
937 the main analysis, though minimal changes around zero are detected for the speed analysis. We
938 reiterate that the magnitudes detected for speed are practically meaningless.

939 Fourth, we show robustness to the definition of our explanatory variable. For each voyage,
940 we calculate the total number of unique encounters that occurred along all previously traveled
941 paths (i.e., surrogate trips), as well as the chosen path, for each port-to-port route within the
942 preceding months of a voyage’s departure. This represents, for any given voyage departure
943 date for any given port-to-port route, the captain’s assessment of the prevalence of piracy along
944 the universe of potential paths that have been recently traveled along the route. We call this
945 variable “Total Number of Encounters.” The results from this test are shown in Figure S10 and
946 are consistent with the main analysis, though there is considerable attenuation. This is expected,
947 as the marginal impact of an additional pirate encounter diminishes as the potential area of paths
948 along a route increases.

949 In addition, for each voyage we calculate the average number of unique attacks that occurred
950 along all previously traveled paths (i.e., surrogate trips) for that port-to-port route within a time
951 window. This represents, for any given voyage departure date for any given port-to-port route,
952 the captain’s expectation of how many attacks they might expect could occur along the route.
953 We call this variable “Average Number of Encounters.” This analysis is presented in Figure S10,

954 and shows considerable attenuation. Positive effects in terms of distance are detected, except
955 in Southeast Asia. Effects in terms of time are mostly dissipated. This result is expected, as it
956 is again easy to see the marginal impact of an additional pirate encounter diminishes further as
957 its effect is now diluted by a considerably increase in the spatial footprint considered, over the
958 number of voyages that took place before.

959 Finally, we show robustness of the results to the addition of speed and days since the last
960 encounter along a route as *covariates*. The results are shown in Figure S11, and are practically
961 unchanged and provide support that the main adjustments are not polluted by not controlling
962 for voyage speed or other short-term features of risk.

table S15: Effect of Past Pirate Encounters on Voyage Distance.

	(1)	(2)	(3)	(4)	(5)	(6)
Encounters (3 mo)	146.59*** (15.40)	134.88*** (14.54)	28.03*** (3.75)	27.17*** (3.56)	26.94*** (3.59)	26.92*** (3.58)
Wind Speed (m/s)		305.58*** (24.57)	43.21*** (4.18)	42.03*** (3.52)	31.54*** (4.77)	31.29*** (4.91)
Wind Resistance Index (m/s) (m/s)		97.15*** (7.85)	11.02*** (1.47)	-2.10** (0.90)	-2.19** (0.94)	-2.78*** (0.90)
Observations	19,478,531	19,475,535	19,475,535	19,475,525	19,475,525	19,475,525
Country Combo. FE			X	X	X	X
Vessel Type FE				X	X	X
Vessel Size FE				X	X	X
Hotspot FE					X	X
Top Route FE						X
Month-by-Year FE	X	X	X	X	X	X

* p < 0.1, ** p < 0.05, *** p < 0.01 The unit of observation is a voyage. The sample spans from 2013 to 2021. Every column is a different specification. Encounters (3mo) is the count of pirate encounters recorded in the projected path of the vessel in the preceding 90 days from the departure date using a 5 degree spatial footprint. Fixed effects include country-to-country combination, vessel type, vessel size, hotspot, and a battery of month by year and top port-to-port combination for country-to-country combination dummies.

table S16: Effect of Past Pirate Encounters on Voyage Time.

	(1)	(2)	(3)	(4)	(5)	(6)
Encounters (3 mo)	7.60*** (0.65)	7.12*** (0.62)	2.29*** (0.33)	2.26*** (0.33)	2.25*** (0.33)	2.25*** (0.33)
Wind Speed (m/s)		12.96*** (0.99)	1.94*** (0.23)	1.91*** (0.21)	1.15*** (0.33)	1.12*** (0.34)
Wind Resistance Index (m/s)		3.72*** (0.36)	0.13** (0.05)	-0.09* (0.05)	-0.10* (0.05)	-0.15*** (0.05)
Observations	19,478,531	19,475,535	19,475,535	19,475,525	19,475,525	19,475,525
Country Combo. FE			X	X	X	X
Vessel Type FE				X	X	X
Vessel Size FE				X	X	X
Hotspot FE					X	X
Top Route FE						X
Month-by-Year FE	X	X	X	X	X	X

* p < 0.1, ** p < 0.05, *** p < 0.01 The unit of observation is a voyage. The sample spans from 2013 to 2021. Every column is a different specification. Encounters (3mo) is the count of pirate encounters recorded in the projected path of the vessel in the preceding 90 days from the departure date using a 5 degree spatial footprint. Fixed effects include country-to-country combination, vessel type, vessel size, hotspot, and a battery of month by year and top port-to-port combination for country-to-country combination dummies.

table S17: Effect of Past Pirate Encounters on Voyage Speed.

	(1)	(2)	(3)	(4)	(5)	(6)
Encounters (3 mo)	0.13*** (0.02)	0.11*** (0.02)	0.01* (0.01)	-0.01* (0.01)	-0.01* (0.01)	-0.01* (0.01)
Wind Speed (m/s)		0.43*** (0.05)	0.09*** (0.02)	0.07*** (0.01)	0.06*** (0.01)	0.06*** (0.01)
Wind Resistance Index (m/s)		0.55*** (0.03)	0.30*** (0.02)	0.01 (0.01)	0.01 (0.01)	0.01 (0.01)
Observations	25,641,468	25,632,270	25,632,270	25,632,233	25,632,233	25,632,233
Country Combo. FE			X	X	X	X
Vessel Type FE				X	X	X
Vessel Size FE				X	X	X
Hotspot FE					X	X
Top Route FE						X
Month-by-Year FE	X	X	X	X	X	X

* p < 0.1, ** p < 0.05, *** p < 0.01 The unit of observation is a voyage. The sample spans from 2013 to 2021. Every column is a different specification. Encounters (3mo) is the count of pirate encounters recorded in the projected path of the vessel in the preceding 90 days from the departure date using a 5 degree spatial footprint. Fixed effects include country-to-country combination, vessel type, vessel size, hotspot, and a battery of month by year and top port-to-port combination for country-to-country combination dummies.

table S18: Effect of Past Pirate Encounters on Fuel Cost.

	(1)	(2)	(3)	(4)	(5)	(6)
Encounters (3 mo)	3.07*** (0.28)	2.83*** (0.27)	0.63*** (0.09)	0.58*** (0.08)	0.58*** (0.08)	0.58*** (0.08)
Wind total (m/s)		6.25*** (0.46)	0.91*** (0.08)	0.80*** (0.08)	0.62*** (0.08)	0.62*** (0.08)
Wind Resistance Index (m/s)		1.99*** (0.15)	0.28*** (0.04)	-0.08*** (0.02)	-0.09*** (0.02)	-0.09*** (0.02)
Observations	25,638,777	25,629,585	25,629,585	25,629,585	25,629,585	25,629,585
Country Combo. FE			X	X	X	X
Vessel Type FE				X	X	X
Vessel Size FE				X	X	X
Hotspot FE					X	X
Top Route FE						X
Month-by-Year FE	X	X	X	X	X	X

* p < 0.1, ** p < 0.05, *** p < 0.01 The unit of observation is a voyage. The sample spans from 2013 to 2021. Every column is a different specification. Encounters (3mo) is the count of pirate encounters recorded in the projected path of the vessel in the preceding 90 days from the departure date using a 5 degree spatial footprint. Fixed effects include country-to-country combination, vessel type, vessel size, hotspot, and a battery of month by year and top port-to-port combination for country-to-country combination dummies.

table S19: Effect of Past Pirate Encounters on Labor Cost

	(1)	(2)	(3)	(4)	(5)	(6)
Encounters (3 mo)	0.99*** (0.09)	0.92*** (0.08)	0.27*** (0.04)	0.26*** (0.03)	0.26*** (0.03)	0.26*** (0.03)
Wind total (m/s)		1.77*** (0.13)	0.28*** (0.03)	0.27*** (0.02)	0.20*** (0.03)	0.20*** (0.03)
Wind Resistance Index (m/s)		0.61*** (0.04)	0.10*** (0.01)	0.00 (0.01)	0.00 (0.01)	-0.01 (0.01)
Observations	25,638,777	25,629,585	25,629,585	25,629,585	25,629,585	25,629,585
Country Combo. FE			X	X	X	X
Vessel Type FE				X	X	X
Vessel Size FE				X	X	X
Hotspot FE					X	X
Top Route FE						X
Month-by-Year FE	X	X	X	X	X	X

* p < 0.1, ** p < 0.05, *** p < 0.01 The unit of observation is a voyage. The sample spans from 2013 to 2021. Every column is a different specification. Encounters (3mo) is the count of pirate encounters recorded in the projected path of the vessel in the preceding 90 days from the departure date using a 5 degree spatial footprint. Fixed effects include country-to-country combination, vessel type, vessel size, hotspot, and a battery of month by year and top port-to-port combination for country-to-country combination dummies.

table S20: Effect of Past Pirate Encounters on Total Cost.

	(1)	(2)	(3)	(4)	(5)	(6)
Encounters (3 mo)	4.06*** (0.36)	3.75*** (0.34)	0.89*** (0.11)	0.84*** (0.11)	0.83*** (0.11)	0.83*** (0.11)
Wind total (m/s)		8.02*** (0.59)	1.18*** (0.11)	1.07*** (0.10)	0.82*** (0.10)	0.82*** (0.11)
Wind Resistance Index (m/s)		2.60*** (0.19)	0.38*** (0.05)	-0.09*** (0.02)	-0.09*** (0.02)	-0.09*** (0.02)
Observations	25,638,777	25,629,585	25,629,585	25,629,585	25,629,585	25,629,585
Country Combo. FE			X	X	X	X
Vessel Type FE				X	X	X
Vessel Size FE				X	X	X
Hotspot FE					X	X
Top Route FE						X
Month-by-Year FE	X	X	X	X	X	X

* p < 0.1, ** p < 0.05, *** p < 0.01 The unit of observation is a voyage. The sample spans from 2013 to 2021. Every column is a different specification. Encounters (3mo) is the count of pirate encounters recorded in the projected path of the vessel in the preceding 90 days from the departure date using a 5 degree spatial footprint. Fixed effects include country-to-country combination, vessel type, vessel size, hotspot, and a battery of month by year and top port-to-port combination for country-to-country combination dummies.

table S21: Effect of Past Pirate Encounters on CO₂ emissions

	(1)	(2)	(3)	(4)	(5)	(6)
Encounters (3 mo)	22.12*** (1.99)	20.39*** (1.89)	3.86*** (0.41)	3.55*** (0.37)	3.50*** (0.37)	3.50*** (0.37)
Wind Speed (m/s)		45.78*** (3.35)	6.52*** (0.55)	5.72*** (0.48)	4.45*** (0.52)	4.46*** (0.52)
Wind Resistance Index (m/s)		14.62*** (1.02)	2.16*** (0.22)	-0.54*** (0.12)	-0.56*** (0.12)	-0.55*** (0.12)
Observations	25,638,777	25,629,585	25,629,585	25,629,585	25,629,585	25,629,585
Country Combo. FE			X	X	X	X
Vessel Type FE				X	X	X
Vessel Size FE				X	X	X
Hotspot FE					X	X
Top Route FE						X
Month-by-Year FE	X	X	X	X	X	X

* p < 0.1, ** p < 0.05, *** p < 0.01 The unit of observation is a voyage. The sample spans from 2013 to 2021. Every column is a different specification. Encounters (3mo) is the count of pirate encounters recorded in the projected path of the vessel in the preceding 90 days from the departure date using a 5 degree spatial footprint. Fixed effects include country-to-country combination, vessel type, vessel size, hotspot, and a battery of month by year and top port-to-port combination for country-to-country combination dummies.

table S22: Effect of Past Pirate Encounters on NO_x Emissions

	(1)	(2)	(3)	(4)	(5)	(6)
Encounters (3 mo)	557.07*** (50.38)	512.92*** (47.69)	94.62*** (10.08)	86.75*** (9.27)	85.69*** (9.28)	85.69*** (9.29)
Wind total (m/s)		1,166.35*** (85.33)	164.94*** (14.01)	144.48*** (12.34)	112.84*** (13.10)	113.01*** (13.05)
Wind Resistance Index (m/s)		370.58*** (25.88)	53.17*** (5.80)	-15.21*** (3.25)	-15.75*** (3.28)	-15.37*** (3.28)
Observations	25,638,777	25,629,585	25,629,585	25,629,585	25,629,585	25,629,585
Country Combo. FE			X	X	X	X
Vessel Type FE				X	X	X
Vessel Size FE				X	X	X
Hotspot FE					X	X
Top Route FE						X
Month-by-Year FE	X	X	X	X	X	X

* p < 0.1, ** p < 0.05, *** p < 0.01 The unit of observation is a voyage. The sample spans from 2013 to 2021. Every column is a different specification. Encounters (3mo) is the count of pirate encounters recorded in the projected path of the vessel in the preceding 90 days from the departure date using a 5 degree spatial footprint. Fixed effects include country-to-country combination, vessel type, vessel size, hotspot, and a battery of month by year and top port-to-port combination for country-to-country combination dummies.

table S23: Effect of Past Pirate Encounters on SO_x Emissions.

	(1)	(2)	(3)	(4)	(5)	(6)
Encounters (3 mo)	460.59*** (41.47)	424.49*** (39.27)	80.34*** (8.47)	73.83*** (7.77)	72.94*** (7.78)	72.94*** (7.79)
Wind total (m/s)		953.21*** (69.77)	135.73*** (11.50)	119.06*** (10.07)	92.71*** (10.81)	92.79*** (10.79)
Wind Resistance Index (m/s)		304.32*** (21.26)	44.97*** (4.62)	-11.25*** (2.49)	-11.70*** (2.52)	-11.51*** (2.52)
Observations	25,638,777	25,629,585	25,629,585	25,629,585	25,629,585	25,629,585
Country Combo. FE			X	X	X	X
Vessel Type FE				X	X	X
Vessel Size FE				X	X	X
Hotspot FE					X	X
Top Route FE						X
Month-by-Year FE	X	X	X	X	X	X

* p < 0.1, ** p < 0.05, *** p < 0.01 The unit of observation is a voyage. The sample spans from 2013 to 2021. Every column is a different specification. Encounters (3mo) is the count of pirate encounters recorded in the projected path of the vessel in the preceding 90 days from the departure date using a 5 degree spatial footprint. Fixed effects include country-to-country combination, vessel type, vessel size, hotspot, and a battery of month by year and top port-to-port combination for country-to-country combination dummies.

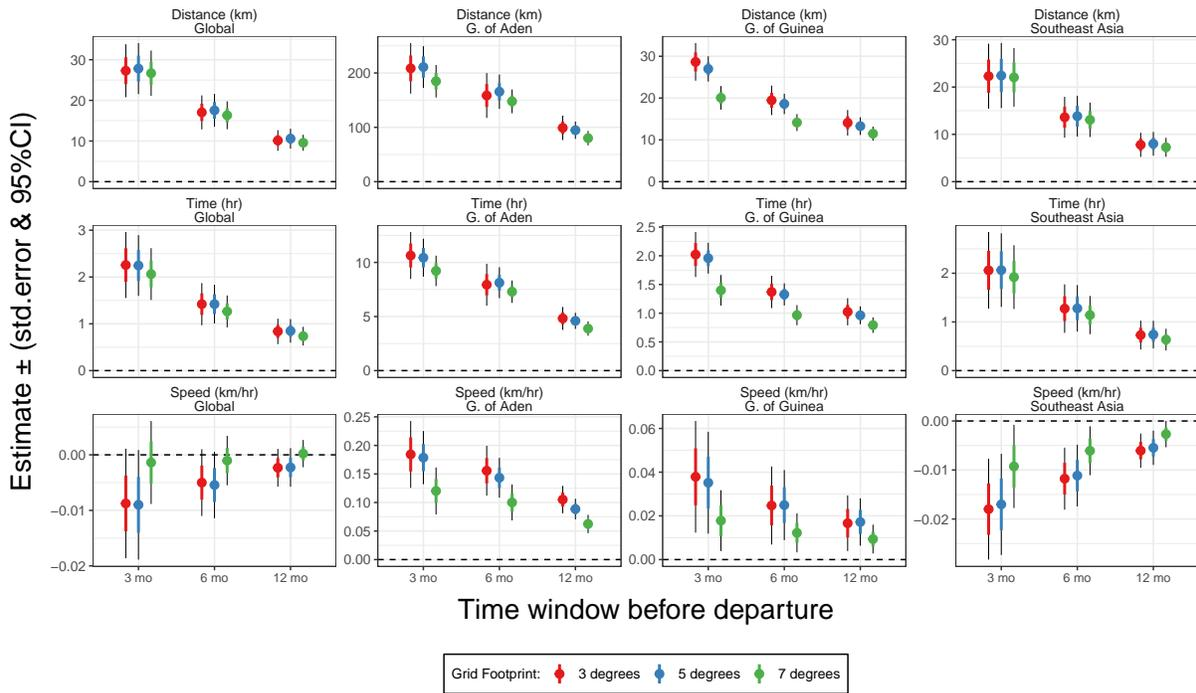


fig S6: Replication Under Different Time Horizons and Degree Footprints. Coefficients show the change in voyage features as a function of the number of pirate encounters in the preceding months. The analysis is conducted for all the variables and subsamples reported in the main text. Each plot shows the results for models using time windows of 3, 6, and 12 months, respectively. Each color shows results for models using a 3, 5, and 7° spatial footprint, respectively. The thick portion of error bars are the clustered standard errors, and the thin portion of error bars shows 95% CIs. Estimation, subsampling, specification, and clustering approach remain identical to those in Table 2.

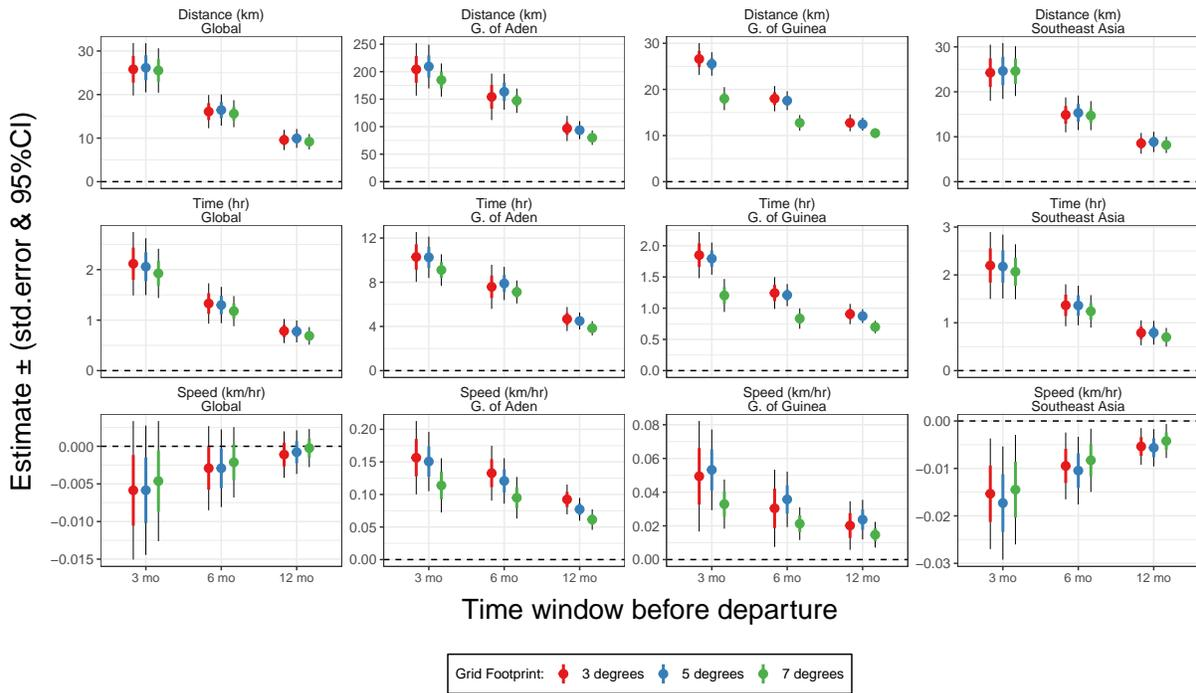


fig S7: **Replication Under Different Time Horizons and Degree Footprints of Vessels Always Classified as Cargo.** Coefficients show the change in voyage features as a function of the number of pirate encounters in the preceding months. The analysis is conducted for all the variables and subsamples reported in the main text. Each plot shows the results for models using time windows of 3, 6, and 12 months, respectively. Each color shows results for models using a 3, 5, and 7° spatial footprint, respectively. The thick portion of error bars are the clustered standard errors, and the thin portion of error bars shows 95% CIs. Estimation, subsampling, specification, and clustering approach remain identical to those in Table 2.

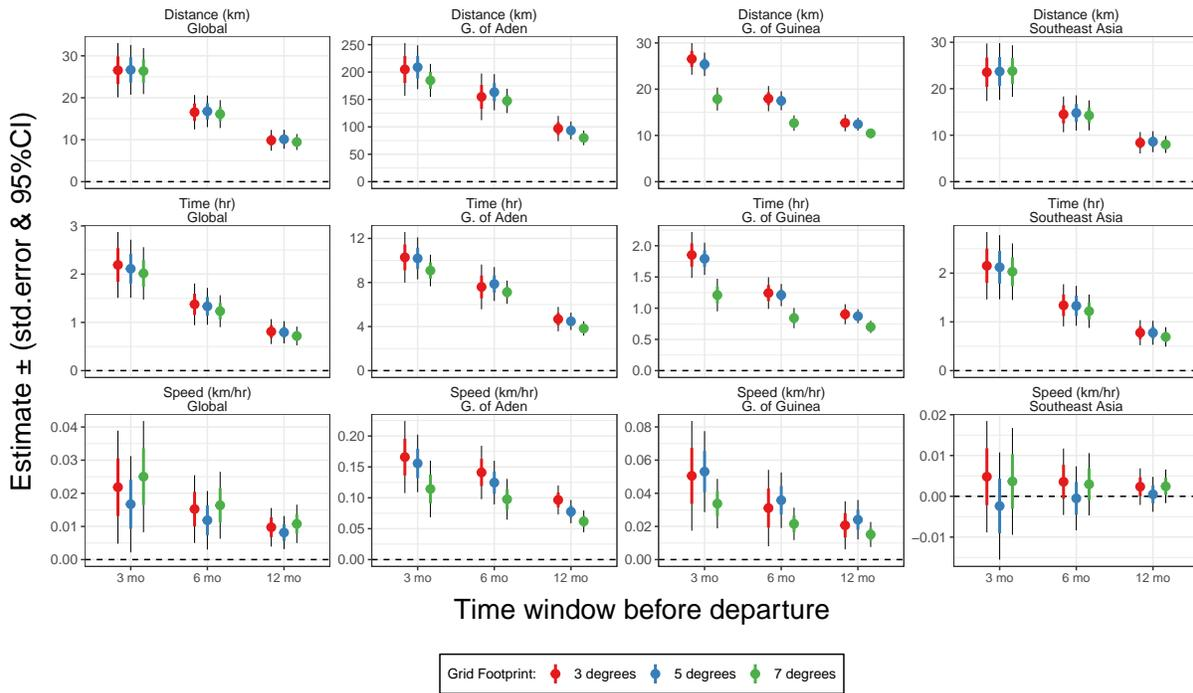


fig S8: **Replication Under Different Time Horizons and Degree Footprints of Vessels at Least Once Classified as Cargo.** Coefficients show the change in voyage features as a function of the number of pirate encounters in the preceding months. The analysis is conducted for all the variables and subsamples reported in the main text. Each plot shows the results for models using time windows of 3, 6, and, 12 months, respectively. Each color shows results for models using a 3, 5, and 7° spatial footprint, respectively. The thick portion of error bars are the clustered standard errors, and the thin portion of error bars shows 95% CIs. Estimation, subsampling, specification, and clustering approach remain identical to those in Table 2.

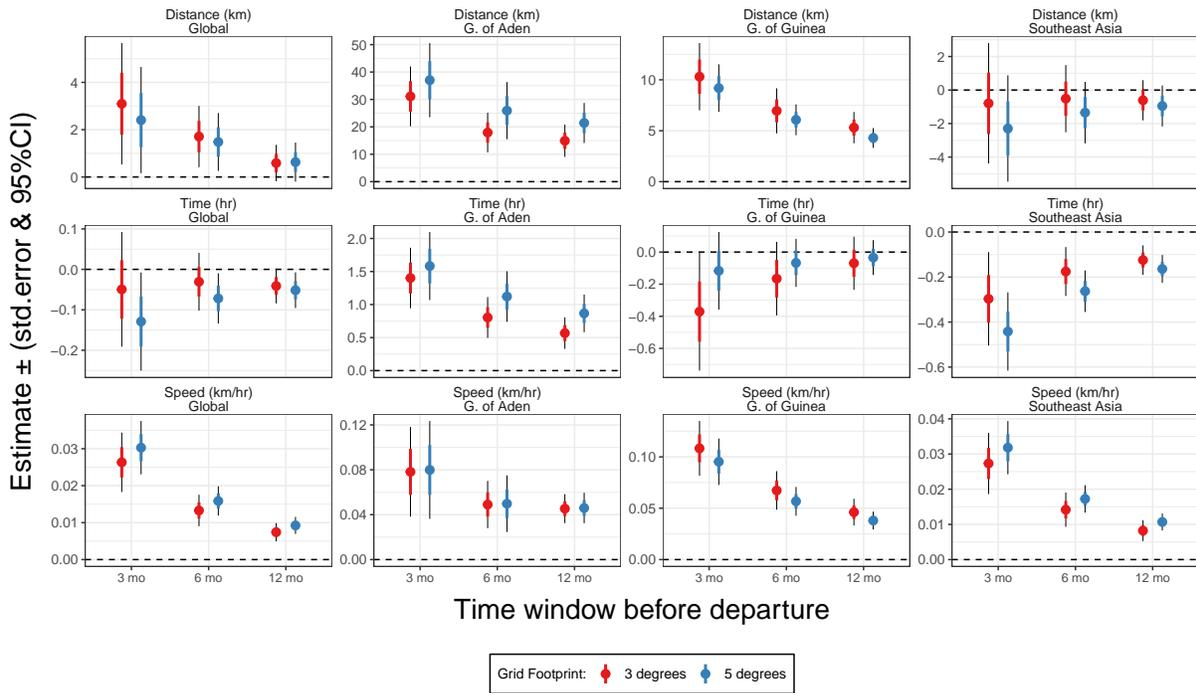


fig S9: Replication Using Average Number of Encounters Under Different Time Horizons and Degree Footprints. Coefficients show the change in voyage features as a function of the average number of pirate encounters experienced by other vessels in the preceding months. The analysis is conducted for all the variables and subsamples reported in the main text. Each plot shows the results for models using time windows of 3, 6, and, 12 months, respectively. Each color shows results for models using a 3 and 5° spatial footprint, respectively. The thick portion of error bars are the clustered standard errors, and the thin portion of error bars shows 95% CIs. Other than the explanatory variable, estimation, subsampling, specification, and clustering approach remain identical to those in Table 2.

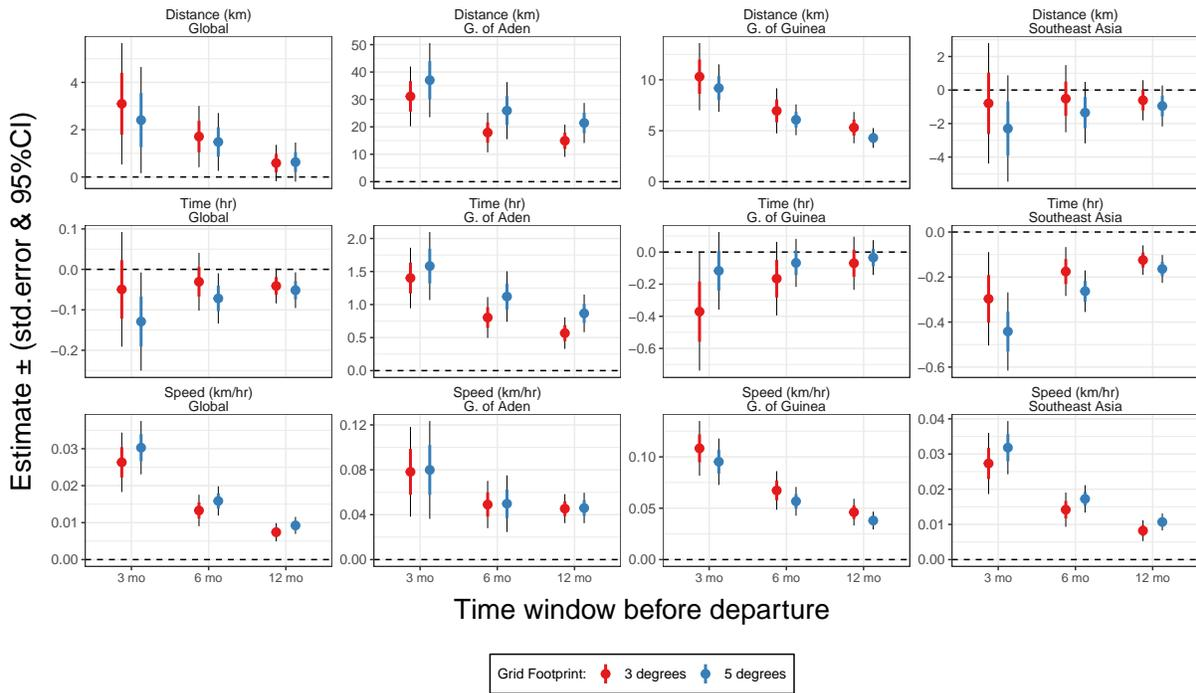


fig S10: Replication Using Total Number of Encounters Under Different Time Horizons and Degree Footprints. Coefficients show the change in voyage features as a function of the average number of pirate encounters experienced by other vessels in the preceding months. The analysis is conducted for all the variables and subsamples reported in the main text. Each plot shows the results for models using time windows of 3, 6, and, 12 months, respectively. Each color shows results for models using a 3 and 5° spatial footprint, respectively. The thick portion of error bars are the clustered standard errors, and the thin portion of error bars shows 95% CIs. Other than the explanatory variable, estimation, subsampling, specification, and clustering approach remain identical to those in Table 2.

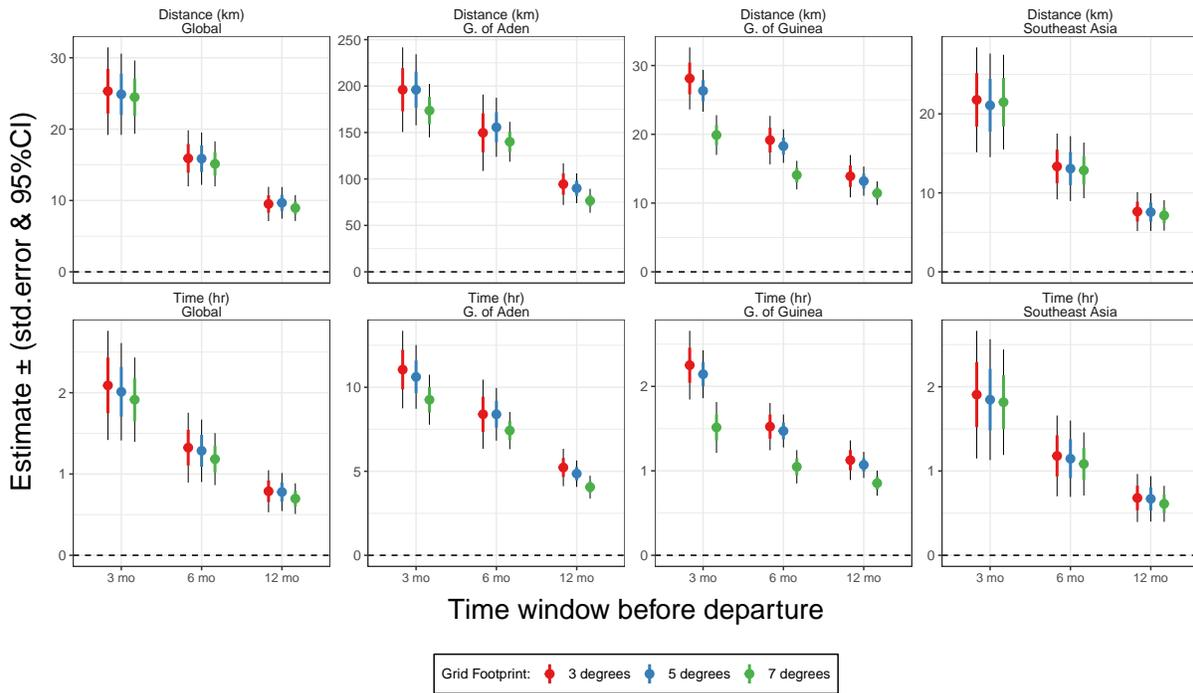


fig S11: **Replication Using Speed and Days Since Last Encounter as Covariates Under Different Time Horizons and Degree Footprints.** Coefficients show the change in voyage features as a function of the average number of pirate encounters experienced by other vessels in the preceding months. The analysis is conducted for all the variables and subsamples reported in the main text. Each plot shows the results for models using time windows of 3, 6, and 12 months, respectively. Each color shows results for models using a 3 and 5° spatial footprint, respectively. The thick portion of error bars are the clustered standard errors, and the thin portion of error bars shows 95% CIs. Other than the explanatory variables, estimation, subsampling, specification, and clustering approach remain identical to those in Table 2.